

DIVERSITY-MULTIPLEXING TRADEOFF FOR NETWORK CODED COOPERATIVE OFDMA SYSTEMS

A Thesis

by

Ali Reza Heidarpour

Submitted to the
Graduate School of Sciences and Engineering
In Partial Fulfillment of the Requirements for
the Degree of

Master of Science

in the
Department of Electrical and Electronics Engineering

Özyeğin University
August 2016

Copyright © 2016 by Ali Reza Heidarpour

DIVERSITY-MULTIPLEXING TRADEOFF FOR NETWORK CODED COOPERATIVE OFDMA SYSTEMS

Approved by:

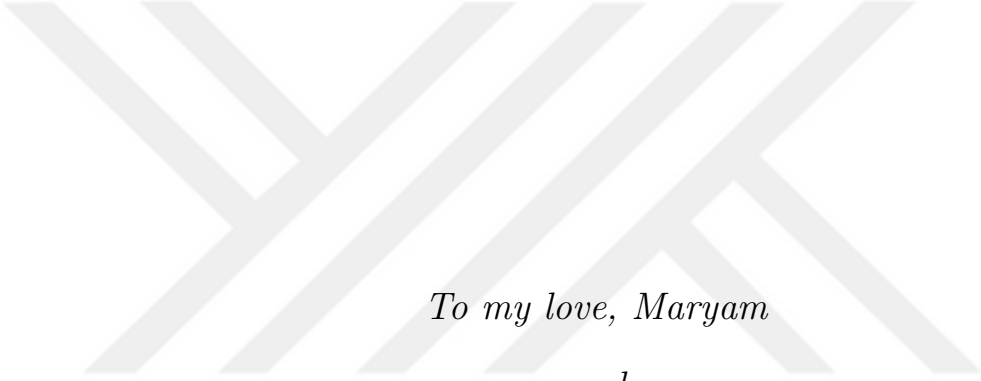


Professor Murat Uysal, Advisor
Department of Electrical and Electronics
Engineering
Özyeğin University

Professor Cenk Demiroglu
Department of Electrical and Electronics
Engineering
Özyeğin University

Professor Gunes Karabulut Kurt
Faculty of Engineering
Istanbul Technical University

Date Approved: 17 August 2016



To my love, Maryam

and

to my dear parents

ABSTRACT

Cooperative communication (CC) exploits the broadcasting nature of wireless transmission and creates a distributed multiple-input multiple-output (MIMO) system among the wireless nodes which are physically separated from each other. Earlier works on cooperative communication typically build on time division multiple access (TDMA). However, it is well known that conventional CC systems experience throughput loss due to additional time slots required for relaying phase which particularly become prohibitive with the increasing number of relay nodes. Network coded cooperative (NCC) systems have been proposed as a powerful alternative with significantly higher throughput efficiency. In an NCC system, the relay nodes perform either XOR operation or form a linear combination of the messages received from distinct sources. Through proper combining, network coding improves the spectral efficiency over conventional unidirectional cooperative communication systems.

In the first chapter of this thesis, we provide an overview of NCC systems and discuss their advantages over conventional CC systems in terms of diversity multiplexing tradeoff (DMT).

All existing works on the DMT analysis of NCC systems assume perfect channel state information (CSI) at relay and destination nodes and focus on asymptotical analysis. It is known that asymptotical DMT analysis overestimates the performance since most communication systems operate in low and moderate signal-to-noise ratio (SNR) regime. To characterize DMT within more practical SNR regime, finite-SNR DMT is a more meaningful performance measure. In the second chapter, we investigate the outage probability and finite-SNR DMT performance for NCC wireless

networks in the presence of imperfect CSI. We show that our results are generalized versions of those earlier presented in the literature and coincide with them in high SNR regime. Our analysis further reveals that the DMT is highly dependent of channel estimation quality particularly at finite-SNR values.

In an effort to have further gains over the initial works, which build upon the assumption of TDMA, the combined use of orthogonal frequency division multiplexing (OFDM) with NCC has been proposed in the literature. In the third chapter, we consider orthogonal frequency division multiple access (OFDMA), an extension of the OFDM to a multiuser system where subsets of carriers are assigned to different users. We derive a closed-form expression for the outage probability of the system over Rayleigh fading channels and present the DMT analysis. Our results demonstrate that NCC-OFDMA system is able to fully exploit both frequency and spatial diversity.

In the third chapter, we investigate only asymptotic DMT analysis of NCC-OFDMA systems over Rayleigh fading channels. In the fourth chapter, we investigate both finite-SNR DMT and asymptotic DMT performance over Rician fading channels. Such an analysis helps us see the difference of performances over Rayleigh and Rician fading channels. Otherwise, DMT results for Rayleigh and Rician channels coincide each other for asymptotical SNR values.

ÖZETÇE

İşbirlikli haberleşme (cooperative communication, CC) kablosuz iletim kanalının doğasında bulunan her yöne yayılım özelliğini kullanır ve fiziksel olarak birbirinden ayrılmış olan kablosuz düğümler arasında dağıtık yapıda bir çok-girişli çok-çıkışlı (multiple-input, multiple-output, MIMO) sistem oluşturur. İşbirlikli haberleşme konusundaki önceki çalışmalar genellikle zaman bölmeli çoklu erişim (time division multiple access, TDMA) tekniği kullanılarak gerçekleştirilmiştir. Bununla birlikte, klasik CC sistemleri aktarma fazındaki iletim için ek zaman aralığı gerektirdiği için birim iletim zamanı başına iletilen veri miktarında kayıba neden olması ile tercih edilmezler. İşbirlikli ağ kodlama (network coded cooperation, NCC) sistemleri ise birim iletim zamanı başına iletilen veri miktarını önemli oranda artırdığı için CC sistemlerine güçlü bir alternatif olarak önerilmiştir. NCC sisteminde röle düğümleri, ayrı kaynak düğümlerinden aldığı mesajların XOR işleminin sonucunu veya doğrusal kombinasyonlarını alıcı düğümlere iletir. Ağ kodlama, uygun birleştirme sayesinde spektral verimliliği geleneksel tek yönlü işbirlikli haberleşme sistemlerine göre artırır.

Bu tezin ilk bölümünde NCC sistemleri ile ilgili genel bilgiler verilip bu sistemlerin çeşitleme ve çoğullama ödünleşimi (diversity and multiplexing tradeoff, DMT) açısından geleneksel CC sistemlerine göre avantajları ortaya konmuştur.

NCC sistemlerinin DMT analizini inceleyen önceki çalışmalarda, kanal durum bilgisinin (channel state information, CSI) röle ve alıcı düğümleri tarafından hatasız olarak bilindiği varsayılmaktadır ve ayrıca sadece asimptotik analizler ele alınmıştır. Haberleşme sistemlerinin büyük bir çoğunluğu düşük ve orta seviyede sinyal-gürültü oranı (signal-to-noise-ratio, SNR) değerlerinde çalışır. Sonlu-SNR için DMT analizi ise pratikte kullanılan SNR aralığındaki DMT analizini gerçekleştirebilmek için daha

anlamli bir basariim olcütüdür. Literatürdeki bu boşluęu gidermek üzere tezin ikinci bölümde NCC sistemlerinin ideal olmayan CSI durumdaki sonlu-SNR DMT analizi gerçekleştirilmiştir. Bu bölümde elde edilen sonuçların literatürdeki çalışmaların genelleştirilmiş halleri olduğu ve yüksek SNR bölgesinde bu çalışmalarla örtüştüğü gösterilmiştir. Ayrıca DMT başarımının kanal kestirim kalitesine baęlı olduğu ortaya konmuştur.

TDMA kullanan önceki çalışmalara göre ek kazanımlar elde etmek için dik frekans bölmeli çoęullama (orthogonal frequency division multiplexing, OFDM) teknięinin NCC sistemlerinde kullanılması literatürde önerilmiştir. Üçüncü bölümde, OFDM çok kullanıcıli sistemlere genişletilmiş hali olan dik frekans bölmeli çoklu erişim (orthogonal frequency multiple access, OFDMA) sistemi ele alınmıştır. Sistemin Rayleigh sönümlemesi altındaki kesinti olasılıęı ifadeleri kapalı formda elde edilmiştir. Elde edilen sonuçlar NCC-OFDMA sisteminin hem frekans hem de uzay çeşitlemesini tam olarak elde edebildiğini göstermiştir.

Tezin üçüncü bölümünde ise NCC-OFDMA sistemine ait asimptotik DMT analizi Rayleigh sönümlemeli kanal için incelenmiştir. Dördüncü bölümde ise hem sonlu-SNR hem de asimptotik DMT başarımlarını Rician sönümlemeli kanallar için ele alınmıştır. Asimptotik SNR deęerleri için elde edilen Rayleigh ve Rician kanallardaki DMT sonuçları birbiriyle örtüşmektedir. Sonlu SNR deęerlerinde ise Rayleigh ve Rician sönümlemeli kanallar arasındaki basariim farkı bu analizler sayesinde ortaya konmuştur.

ACKNOWLEDGEMENTS

First, I am thankful to Allah, the most merciful and most compassionate for the strengths and His blessing in completing this work.

Second, I would like to express my deepest and profound gratitude to my supervisor, Prof. Murat Uysal for providing consistent guidance, motivation and support throughout my master studies. I have no doubt that without his insightful suggestions and advices, I could never come thus far. I would like to thank my thesis committee members, Professors Gunes Karabulut Kurt, and Cenk Demiroglu who despite their busy schedules accepted to review my thesis.

Finally, and most importantly, I thank my parents, and my wife for their love, kindness, and prayers during the course of my MSc.

This work is supported by TUBITAK under Grant 113E294.

TABLE OF CONTENTS

DEDICATION	iii
ABSTRACT	iv
ÖZETÇE	vi
ACKNOWLEDGEMENTS	viii
LIST OF TABLES	xi
LIST OF FIGURES	xii
I INTRODUCTION	1
II FINITE-SNR DMT ANALYSIS FOR NCC SYSTEMS WITH IMPERFECT CSI	7
2.1 System Model	7
2.2 Finite-SNR DMT Analysis	9
2.3 Numerical Results and Discussion	14
III ASYMPTOTIC DIVERSITY-MULTIPLEXING TRADEOFF FOR NETWORK CODED COOPERATIVE OFDMA SYSTEMS OVER RAYLEIGH FADING CHANNELS	19
3.1 System Model	19
3.2 Derivation of Outage Probability	22
3.2.1 The Outage Probability for Subcarriers	22
3.2.2 The Overall Outage Probability of System	23
3.3 Diversity-Multiplexing Tradeoff Analysis	25
3.4 Numerical Results and Discussion	28
IV FINITE-SNR DIVERSITY-MULTIPLEXING TRADEOFF FOR NETWORK CODED COOPERATIVE OFDMA SYSTEMS OVER RICIAN FADING CHANNELS	32
4.1 System Model	32
4.2 Derivation of Outage Probability	33
4.2.1 Outage Probability for Subcarriers	33

4.2.2	Overall Outage Probability	34
4.3	DMT Analysis	34
4.3.1	Derivation of Asymptotical DMT	34
4.3.2	Derivation of Finite-SNR DMT	36
4.3.3	Asymptotic Behavior of Finite-SNR DMT	38
4.3.4	Finite-SNR Diversity Gain for a Fixed transmission Rate . .	39
4.4	Numerical Results and Discussion	41
V	CONCLUSION	48
	REFERENCES	49
	VITA	52

LIST OF TABLES



LIST OF FIGURES

1	DMT comparison for different cooperative communication protocols. .	3
2	NCC system with P source nodes, M relay nodes, and one destination. Solid lines: broadcasting phase. Dashed lines: relaying phase. Relay nodes which decode all the packets from P source nodes correctly are allowed to participate in relaying phase.	8
3	Outage probability of NCC system for different number of relay nodes under imperfect CSI.	15
4	Finite-SNR diversity gain versus SNR.	16
5	Finite-SNR diversity gain versus δ	17
6	Finite-SNR DMT for different values of SNR under imperfect CSI. . .	18
7	DMT comparison of stand-alone OFDMA and NCC-OFDMA systems ($P > M$).	27
8	Outage probability for NCC-OFDMA for different values of R_0	28
9	Outage probability of NCC-OFDMA for different values of P	29
10	Outage probability of NCC-OFDMA for different values of M	30
11	Outage probability for NCC-OFDMA for different values of L	30
12	Outage probability for different values of M	42
13	Diversity gain for different values of M at fixed transmission rate. . .	43
14	Diversity gain for different values of L at fixed transmission rate. . . .	44
15	Diversity gain for different values of fixed transmission rate.	44
16	Diversity gain for different values of P at fixed transmission rate. . .	45
17	Finite-SNR DMT for different values of M	46
18	Finite-SNR DMT for different values of SNR.	47

CHAPTER I

INTRODUCTION

Cooperative communication (CC) [1–3], also referred as cooperative diversity, is an effective approach to exploit spatial diversity when the deployment of multiple antennas is not feasible. CC takes advantage of the broadcasting nature of wireless transmission and creates virtual multiple-input multiple-output (MIMO) channels among the nodes willing to share their resources with each other [4]. Conventional CC systems build upon time division multiple access (TDMA) and experience throughput loss due to additional time slots required for relaying phase. Inspired by the earlier work on network coding in [5] for wired networks, network coded cooperation (NCC) has been proposed [6–8] to address the throughput efficiency in wireless networks. In NCC, the relay nodes perform a combining operation (which takes the form of XOR or linear combinations) on the data received from distinct sources and send the resulting signal to the destination. This method reduces the total transmission time and improves the spectral efficiency over conventional CC.

In [9], Peng et al. consider N source-destination pairs and M relay nodes with dynamic coding (DC-NCC). Particularly, the best relay (which has the best end-to-end path between source and destination) among the set of M available relay nodes are selected and then the relay dynamically employs XOR operation on the source packets based on instantaneous source to relay channel quality. It is shown that the DC-NCC system can achieve a full diversity gain of $M + 1$. However, diversity gain of $M + 1$ can only be obtained under the assumption where the destination can successfully overhear the data from other source nodes. If this optimistic assumption is removed, the achievable diversity gain of the DC-NCC system reduces to only two

and does not improve by increasing the number of relay candidates. In an effort to improve the diversity gains, random NCC (RNCC) system and deterministic NCC (DNCC) system are presented in [10], where relay nodes encode the sources packets using an encoding matrix of size $(N+M) \times N$. In this set-up, the first N rows form an identity sub-matrix, corresponding to the direct transmission in broadcasting phase. In addition, the remaining columns and rows correspond to the packets transmitted by relays in relaying phase. In DNCC system the coefficients in encoding matrix are preset while in RNCC system are drawn randomly from finite field. The associated DMT analysis reveals that a full diversity gain of $M+1$ can be maintained through the use of maximum distance separable (MDS) codes typically used for point to point channels.

Diversity-multiplexing tradeoff (DMT) determines the set of diversity and multiplexing gain pairs that can be obtained simultaneously. Fig. 1 depicts diversity gain d versus multiplexing gain r for different cooperative communication protocols. It is known that CC systems including space-time coding [11] and opportunistic relaying [12] achieve the same DMT of $d(r) = (M+1)(1-2r)$, $r \in (0, 0.5)$ while [12] does not require coordination and space-time coding among relay nodes. The DMT expressions of DC-NCC and DNCC/RNCC systems are given in [10]. As can be seen from Fig. 1, CC and RNCC/DNCC systems can achieve full diversity gain of $M+1$ when $r=0$. However, DNCC/RNCC systems outperform CC systems in terms of multiplexing gain and offer higher diversity gain than that of CC systems for the same spectral efficiency. On the other hand, in comparison to other schemes, DC-NCC system has the highest multiplexing gain and offers more diversity gain as r increases. This is due to the fact that only one relay XORs source packets and therefore the overall transmission takes place in $N+1$ orthogonal time slots. It is worth mentioning that as N increases the spectral efficiency of the NCC systems moves towards the ideal case. Therefore, NCC systems have better DMT performance and outperform CC

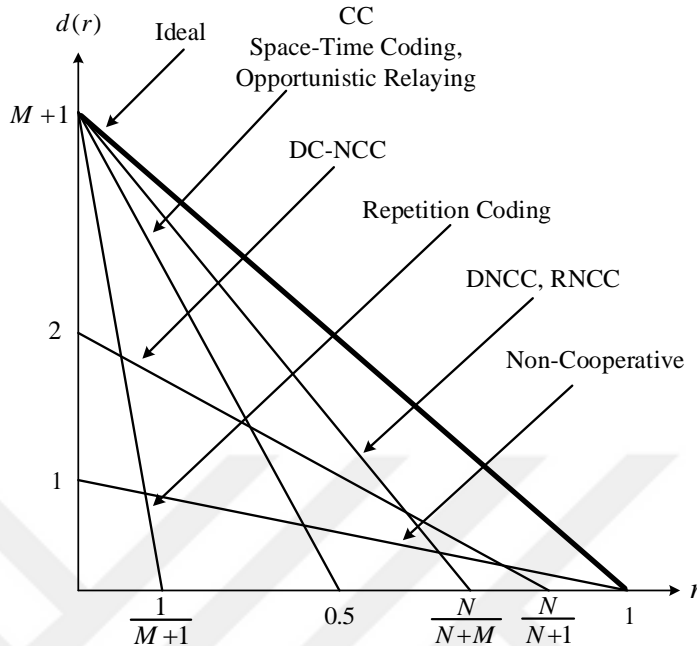


Figure 1: DMT comparison for different cooperative communication protocols.

systems.

In contrast to majority of the existing works on NCC which build upon the assumption of TDMA, the use of orthogonal frequency division multiplexing (OFDM) with NCC is explored in [13–15]. NCC-OFDM achieves high spectral efficiency and requires low complexity receivers. These initial works present performance evaluation of NCC-OFDM with a focus either on bit error rate [13] or network throughput [14]. Some other works also address optimal resource allocation to maximize the sum capacity [15] or weighted sum rate [16].

Some related works which focus on the DMT analysis of stand-alone OFDM(A) systems are also worth mentioning. For example, in [17–19] the DMT analysis of OFDM system is investigated. In [20], Bai *et al.* consider multi-user setting and show that the maximum diversity gain of an OFDMA system with a judiciously designed subcarrier allocation scheme is the same as that of point-to-point OFDM system. Another DMT analysis of OFDMA systems is presented in [21] and the

so-called maximum constraint $\kappa_{1,K}$ -matching approach (MCMA) is proposed as an optimal subcarrier allocation method.

The derivation of conventional DMT assumes asymptotically high signal-to-noise ratio (SNR), i.e., when SNR goes to infinity. For characterizing DMT within more practical SNR range, finite-SNR DMT is proposed in [22–24]. Furthermore, finite-SNR analysis is essential to observe the possible performance differences among various fading channel types [23]. Finite-SNR analysis has already been applied to various bidirectional communication protocols [25–31]. In [25], Liu and Kim investigate finite-SNR DMT of three different bidirectional protocols namely time-division broadcast (TDBC), physical-layer network coding (PNC), and opportunistic source selection (OSS). It is shown that TDBC and OSS protocols outperform PNC and two-phase analog network coding (ANC) [26–28] in terms of diversity gains. On the other hand, PNC and two-phase (ANC) require only two time slots to exchange one information symbol and therefore, achieve higher multiplexing gains. To further increase diversity gain of ANC, three-phase ANC is proposed in [29] which takes advantage of direct link between two source nodes. Asymptotical and finite-SNR DMT analysis of three-phase ANC can be found in [30] and [31] respectively.

This thesis makes several contributions to the information theoretical performance analysis of NCC systems. More specifically, all existing works on the DMT analysis of NCC systems assume perfect channel state information (CSI) at relay and destination nodes and focus on asymptotical analysis. It is known that asymptotical DMT analysis overestimates the performance since most communication systems operate in low and moderate SNR regime. In the first part of the thesis, we investigate the outage probability and finite-SNR DMT performance for NCC systems in the presence of imperfect CSI. We show that our results are generalized versions of those earlier presented in [10] and coincide with them in high SNR regime. Our analysis further reveals that the DMT is highly dependent of channel estimation quality particularly

at finite-SNR values.

In the second part of the thesis, we extend the DMT analysis of [10] presented for single-carrier TDMA-based NCC systems to orthogonal frequency division multiple access (OFDMA), an extension of the OFDM to a multiuser system where subsets of carriers are assigned to different users. We derive the outage probability of the system over Rayleigh fading channel and present the asymptotic DMT analysis. Our results demonstrate that NCC-OFDMA system is able to fully exploit both frequency and spatial diversity. Since asymptotical DMT of Rayleigh and Rician fading channels are identical, we characterize DMT for finite SNRs of practical relevance. As opposed to Rayleigh fading, over Rician fading channels, the maximum diversity gain is not achieved at zero multiplexing gain. It can be observed from our results that the presence of line-of-sight (LOS) components in Rician fading leads diversity gains higher than asymptotic SNR values at some multiplexing gains and SNRs.

The rest of the thesis is organized as follows: In Chapter II, we investigate the information theoretical limits of NCC systems in the presence of imperfect CSI. We derive exact outage probability and finite-SNR DMT for NCC wireless networks over Rayleigh fading channels. In Chapter III, we investigate asymptotic DMT analysis of NCC-OFDMA systems over Rayleigh fading channels. In Chapter IV, we investigate both finite-SNR DMT and asymptotic DMT performance over Rician fading channels. Finally, we conclude in Chapter V.

Notation: In this paper, $\ln(\cdot)$, and $E[\cdot]$ denote natural logarithm, and expectation operator respectively. $\Pr\{\cdot\}$, $(\cdot)^T$, $\binom{\cdot}{\cdot}$, $\|\cdot\|$, and \approx denote probability, matrix transpose, binomial coefficient, cardinality of the set, and approximate equality, respectively. $\lfloor \cdot \rfloor$ denotes the floor function. $\mathcal{CN}(0, 1)$ represents circularly symmetric complex Gaussian random variable with zero mean and variance one. Let $F = \{f_1, \dots, f_N\}$ denote the set of subcarriers where f_n is the n^{th} subcarrier. $Q_1(\cdot, \cdot)$ and $I_n(\cdot)$ respectively, are Marcum Q -function of order one and n^{th} order modified

Bessel function of the first kind.



CHAPTER II

FINITE-SNR DMT ANALYSIS FOR NCC SYSTEMS WITH IMPERFECT CSI

In this chapter, we investigate the performance of general multisource multirelay NCC systems in the presence of imperfect CSI. Based on the derived outage probability, we obtain closed-form expression for finite-SNR DMT. Our results reveal that at practical channel estimation quality and SNR regime, the DMT of the system is substantially less than that of asymptotic one. This analysis can be useful to predict the performance of NCC system under realistic operating conditions taking into account channel estimation errors and finite SNR regime.

2.1 *System Model*

We consider an NCC system with P source nodes S_i , ($i = 1, \dots, P$), M relay nodes R_j , ($j = 1, \dots, M$), and a single destination D as shown in Fig. 2. During the first phase, source nodes broadcast their packets I_i , ($i = 1, 2, \dots, P$) to the destination in P orthogonal time slots and relay nodes overhear transmissions. During the second phase, the source nodes remain silent and relay nodes transmit their packets I'_j , ($j = 1, 2, \dots, M$) to the destination. Relay nodes encode the sources' packets using an encoding matrix \mathbf{Z} given by

$$\mathbf{Z} = \left(\begin{array}{cccc|ccc} 1 & 0 & \cdots & 0 & \alpha_{1,1} & \cdots & \alpha_{M,1} \\ 0 & 1 & \cdots & 0 & \alpha_{1,2} & \cdots & \alpha_{M,2} \\ \vdots & \vdots & \ddots & \vdots & \vdots & \ddots & \vdots \\ 0 & 0 & \cdots & 1 & \alpha_{1,M} & \cdots & \alpha_{M,P} \end{array} \right)_{P \times (P+M)}^T, \quad (1)$$

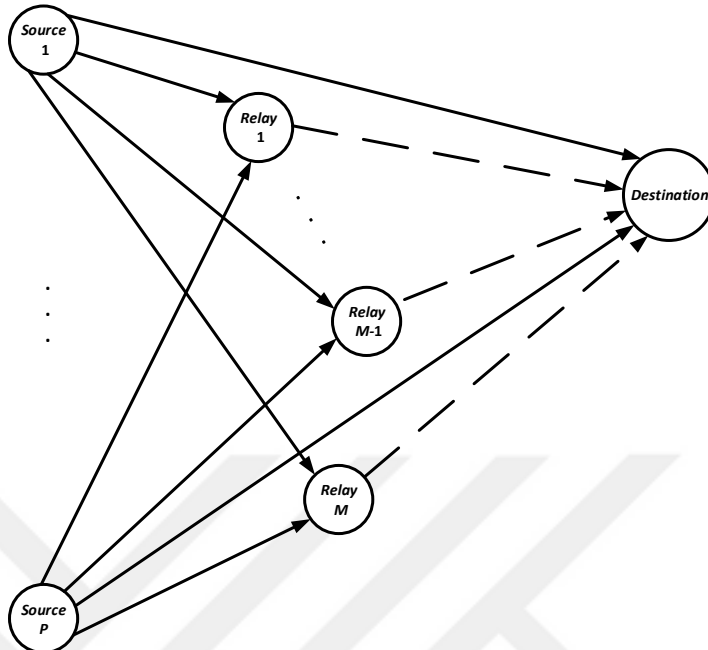


Figure 2: NCC system with P source nodes, M relay nodes, and one destination. Solid lines: broadcasting phase. Dashed lines: relaying phase. Relay nodes which decode all the packets from P source nodes correctly are allowed to participate in relaying phase.

where the first P rows of \mathbf{Z} form an $P \times P$ identity sub-matrix, corresponding to the direct source to destination transmission links in broadcasting phase. The remaining columns and rows correspond to the packets transmitted by relays. We assume that only the relays which successfully decode all of their received packets from P source nodes are allowed to participate in the relaying phase. Assume that m out of M relays do not decode all P packets correctly. Therefore, the rows of \mathbf{Z} which correspond to these m relays with erroneous decisions are deleted. Practically, this can be determined through the use of error detection codes such as cyclic redundancy check (CRC). It is assumed that relays and destination are able to decode packets correctly if source-to-destination, source-to-relay, and relay-to-destination links are not in outage.

The channel between any pair of nodes is identically independent quasi-static Rayleigh fading. Let h_{XY} , $XY \in \{S_i D, S_i R_j, R_j D\}$ denote the channel gain of $X \rightarrow$

Y link, which is circular symmetric complex Gaussian random variable with zero mean and variance $\sigma_{h_{XY}}^2 = 1$. The envelope of h_{XY} follows Rayleigh distribution. We assume that each node has a transmit power P_t and the noise for each link is additive white Gaussian noise (AWGN) with zero mean and variance of N_0 . We assume linear minimum mean-square error (LMMSE) channel estimation at the receiver side. Therefore the received signal from link $X \rightarrow Y$ is given by

$$y_{XY} = \sqrt{P_t} (\hat{h}_{XY} + e_{XY}) x_{XY} + w_{XY}, \quad (2)$$

where x_{XY} is the symbol transmitted from link $X \rightarrow Y$ and w_{XY} is AWGN. In (2), \hat{h}_{XY} is the estimated version of h_{XY} and e_{XY} is the channel estimation error and independent of \hat{h}_{XY} . This is a valid assumption for LMMSE estimation where the estimate and the error are orthogonal. Note that the term $\sqrt{P_t} e_{XY} x_{XY}$ can be interpreted as either additional signal power or AWGN. The former interpretation yields upper bound of channel capacity while the latter can be used to obtain the lower bound of channel capacity [32]. As discussed in [33], under the assumption that channel estimation error power contributes as an additional signal power, the upper bound is a loose bound since it can take a large value even when \hat{h}_{XY} is near zero. Therefore, similar to the approach followed in [28,31], we assume that the channel estimation error acts like AWGN/interference, where it cannot be properly detected and be exploited as signal throughout the communication process. The variance of the estimation error is given by $\sigma_{e_{XY}}^2 = \sigma_{h_{XY}}^2 / (1 + \delta \rho \sigma_{h_{XY}}^2) = 1 / (1 + \delta \rho)$ [33], where $\rho = P_t / N_0$ is the average transmit SNR and $\delta > 0$ reflects the quality of the CSI and depends on the training duration and the training SNR [28,31,33,34]. In this case, the variance of \hat{h}_{XY} can be expressed as $\sigma_{\hat{h}_{XY}}^2 = \sigma_{h_{XY}}^2 - \sigma_{e_{XY}}^2 = \delta \rho \sigma_{h_{XY}}^4 / (1 + \delta \rho \sigma_{h_{XY}}^2) = \delta \rho / (1 + \delta \rho)$.

2.2 *Finite-SNR DMT Analysis*

The outage probability of the $X \rightarrow Y$ link is given by

$$P_{out} = \Pr \{ \log_2 (1 + \gamma_{XY}) < R_0 \}, \quad (3)$$

where $R_0 = (P + M)R/P$ is the transmission rate and R is the system rate [10]. Based on (2), the instantaneous received SNR over the link $X \rightarrow Y$ is obtained as $\gamma_{XY} = P_t |\hat{h}_{XY}|^2 / (P_t \sigma_{e_{XY}}^2 + N_0)$. The average received SNR can be then expressed as

$$\mathbb{E}[\gamma_{XY}] = \bar{\gamma}_{XY} = \frac{P_t \sigma_{\hat{h}_{XY}}^2}{P_t \sigma_{e_{XY}}^2 + N_0} = \frac{\delta \rho^2}{(1 + \delta) \rho + 1}. \quad (4)$$

Let r_f denote the finite-SNR multiplexing gain. Replacing $R(\rho) = r_f \log_2(1 + \rho)$ [22] in (3) and noting that the CDF of γ_{XY} under Rayleigh fading assumption is given by $F_{\gamma_{XY}}(y) = 1 - \exp(-y/\bar{\gamma}_{XY})$, we have

$$P_{out} = 1 - \exp(-\vartheta), \quad (5)$$

where $\vartheta = \left((1 + \rho)^{(P+M)r_f/P} - 1 \right) \left((1 + \delta) \rho + 1 \right) / (\delta \rho^2)$.

In NCC system, if the destination is able to decode at least P packets from out of $P+M$ potential packets transmitted in broadcasting and relaying phases, it is capable to recover all original packets, otherwise it is in outage. The outage probability of the system under consideration is given by

$$P_o(r_f, \rho) = \underbrace{\sum_{m=0}^M \binom{M}{m} P_c^{M-m} (1 - P_c)^m}_{\Theta_1} \times \underbrace{\sum_{j=0}^{P-1} \binom{P+M-m}{j} P_{out}^{P+M-m-j} (1 - P_{out})^j}_{\Theta_2}, \quad (6)$$

where P_c is the probability that any relay successfully decodes all P packets received during the broadcasting phase and expressed as $P_c = (1 - P_{out})^P = \exp(-P\vartheta)$. In (6), Θ_1 denotes the probability of all possible events that m out of M relays are in outage and Θ_2 denotes the probability of all possible events that at most $P - 1$ nodes from P source nodes and $M - m$ participating relays are not in outage.

The finite-SNR DMT is given by [22]

$$d_f(r_f, \rho) = -\frac{\partial \ln(P_o(r_f, \rho))}{\partial \ln(\rho)} = -\frac{\rho}{P_o(r_f, \rho)} \frac{\partial P_o(r_f, \rho)}{\partial \rho}. \quad (7)$$

Inserting (6) in (7), for the second term of (7), we have

$$\frac{\partial P_o(r_f, \rho)}{\partial \rho} = \Theta_2 \frac{\partial \Theta_1}{\partial \rho} + \Theta_1 \frac{\partial \Theta_2}{\partial \rho}. \quad (8)$$

Taking derivative of Θ_1 and Θ_2 with respect to ρ , we respectively have

$$\begin{aligned} \partial \Theta_1 / \partial \rho &= \sum_{m=0}^M \binom{M}{m} \partial P_c / \partial \rho P_c^{M-m-1} (1 - P_c)^{m-1} \\ &\quad \times (-m + M(1 - P_c)), \end{aligned} \quad (9)$$

$$\begin{aligned} \partial \Theta_2 / \partial \rho &= \sum_{j=0}^{P-1} \binom{P+M-m}{j} \partial P_{out} / \partial \rho P_{out}^{P+M-m-j-1} \\ &\quad \times (1 - P_{out})^{j-1} (P + M - m - j - (P + M - m) P_{out}). \end{aligned} \quad (10)$$

In (9) and (10) we have

$$\partial P_c / \partial \rho = -P \exp(-P\vartheta) \partial \vartheta / \partial \rho, \quad (11)$$

$$\partial P_{out} / \partial \rho = \exp(-\vartheta) \partial \vartheta / \partial \rho, \quad (12)$$

where $\partial \vartheta / \partial \rho$ is given by

$$\begin{aligned} \frac{\partial \vartheta}{\partial \rho} &= \frac{\frac{P+M}{P} r_f (1 + \rho)^{\frac{P+M}{P} r_f - 1} ((1 + \delta) \rho + 1) + (1 + \delta) \left((1 + \rho)^{\frac{P+M}{P} r_f} - 1 \right)}{\delta \rho^2} \\ &\quad - \frac{2 \left((1 + \rho)^{\frac{P+M}{P} r_f} - 1 \right) ((1 + \delta) \rho + 1)}{\delta \rho^3}. \end{aligned} \quad (13)$$

After some mathematical manipulations and substituting (8) into (7), we obtain the finite-SNR DMT given by

$$d_f(r_f, \rho) = \frac{1}{P_o(r_f, \rho)} \left[\underbrace{\sum_{m=0}^M \binom{M}{m} P \vartheta \exp(-P\vartheta) \Lambda P_c^{M-m-1} (1-P_c)^{m-1} (m-M(1-P_c)) \Theta_2}_{v_1} + \underbrace{\sum_{j=0}^{P-1} \binom{P+M-m}{j} \vartheta \exp(-\vartheta) \Lambda P_{out}^{P+M-m-j-1} (1-P_{out})^{j-1} (P+M-m-j-(P+M-m)P_{out}) \Theta_1}_{v_2} \right], \quad (14)$$

where Λ is given by

$$\Lambda = 2 - \frac{\frac{P+M}{P} r_f (1+\rho)^{\frac{P+M}{P} r_f - 1} ((1+\delta)\rho + 1) \rho + (1+\delta) \left((1+\rho)^{\frac{P+M}{P} r_f} - 1 \right) \rho}{\left((1+\rho)^{\frac{P+M}{P} r_f} - 1 \right) ((1+\delta)\rho + 1)}. \quad (15)$$

In the following, we discuss the effect of channel estimation on the finite-SNR DMT. It should be noted that the limiting diversity gain as $r_f \rightarrow 0$ is not meaningful since the channel estimation error variance contributes to nonzero mutual information irrespective of the fading realization [33]. However it is worth studying the impact of the channel estimation quality on limiting behavior of DMT at zero multiplexing gain (i.e., $r_f \rightarrow 0$).

When $r_f \rightarrow 0$, ϑ goes to zero which yields $\lim_{\vartheta \rightarrow 0} P_{out} = \vartheta$, and $\lim_{\vartheta \rightarrow 0} (1-P_c) = P\vartheta$. After some mathematical manipulations, we obtain

$$\lim_{\vartheta \rightarrow 0} P_o(r_f, \rho) = \xi \vartheta^{M+1}, \quad (16)$$

where $\xi = \sum_{m=0}^M \binom{P+M-m}{P-1} \binom{M}{m} P^m$.

Now consider the remaining term of (14). It can be checked that $\lim_{r_f \rightarrow 0} \Lambda$ has indeterminate form. Applying L'Hopital's rule, $\lim_{r_f \rightarrow 0} \Lambda = \tilde{\Lambda}$ can be expressed as

$$\tilde{\Lambda} = 2 - \frac{((1 + \delta)\rho + 1)\rho(1 + \rho)^{-1} + (1 + \delta)\rho \ln(1 + \rho)}{((1 + \delta)\rho + 1)\ln(1 + \rho)}. \quad (17)$$

Similar to (16), by considering the smallest order of ϑ for the other terms, we have

$$\lim_{\vartheta \rightarrow 0} v_1 = \xi \vartheta^{M+1} \tilde{\Lambda} m, \quad (18)$$

and

$$\lim_{\vartheta \rightarrow 0} v_2 = \xi \vartheta^{M+1} \tilde{\Lambda} (M - m + 1). \quad (19)$$

Finally we obtain

$$\lim_{r_f \rightarrow 0} d_f(r_f, \rho) = (M + 1) \left(2 - \frac{((1 + \delta)\rho + 1)\rho(1 + \rho)^{-1} + (1 + \delta)\rho \ln(1 + \rho)}{((1 + \delta)\rho + 1)\ln(1 + \rho)} \right). \quad (20)$$

It is observed that the diversity gain is given by the product of $M + 1$ and a term which is function of the channel estimation error and SNR. This term can be less than 1. Thus, it can be seen that zero multiplexing gain does not always give maximum diversity gain.

Special case (Perfect CSI): When $\delta \rightarrow \infty$ i.e., no estimation error, (20) reduces to

$$\lim_{\substack{r_f \rightarrow 0 \\ \delta \rightarrow \infty}} d_f(r_f, \rho) = (M + 1) \left(1 - \frac{\rho}{(1 + \rho)\ln(1 + \rho)} \right). \quad (21)$$

For $\rho \rightarrow \infty$, i.e., asymptotical SNR regime, both (20) and (21) reduces to $M + 1$ indicating that full diversity is achieved. This is due to the fact that channel estimation errors tend to zero as the SNR goes to infinity. In this case, in asymptotical

SNR regime channel estimation errors does not impact on the diversity gain and full diversity gain can be obtained.

Special case (Asymptotical SNR): In this section, we investigate the asymptotical DMT. For $\rho \rightarrow \infty$, we have $\lim_{\rho \rightarrow \infty} \vartheta = (1 + \delta) \rho^{((P+M)r/P)-1} / \delta$. Noting that $r < P/(P + M)$ [10], we obtain $\vartheta \rightarrow 0$. In addition, $\lim_{\rho \rightarrow \infty} \Lambda = 1 - (P + M)r/P$. Following similar steps for obtaining (20), we have

$$\lim_{\rho \rightarrow \infty} d_f(r_f, \rho) = d(r) = (M + 1) \left(1 - \frac{P + M}{P} r \right), \quad (22)$$

where the maximum diversity gain is obtained for $r = 0$ i.e., $M + 1$. On the other hand the maximum multiplexing gain $P/(P + M)$ is achieved when $d(r) = 0$. In fact, (21) coincides to asymptotical DMT expression derived in [10] under the assumption of perfect CSI. This is due to the fact that the channel estimation errors tend to zero in high SNR regime and do not affect on the DMT expression. It can be easily checked that for zero multiplexing gain ($r = 0$), (22) will be equal to (20) when $\rho \rightarrow \infty$.

2.3 Numerical Results and Discussion

In this section, we present numerical results as well as Monte-Carlo simulations to confirm the accuracy of our derivations.

Fig. 3, depicts the outage probability of NCC system for different number of relay nodes and channel estimation errors. We assume $P = 4$ source nodes, $R_0 = 0.2$, $M = 2, 3$ relay nodes, and $\delta = 0.4, 2$. As a benchmark, perfect CSI (i.e., $\delta \rightarrow \infty$) is also plotted. It can be seen that the derived expressions in (6) matched well with simulation results confirming the accuracy of derivations. It is observed that channel estimation quality significantly impacts the outage performance. For example, to achieve an outage probability of 10^{-6} for $M = 2$, an SNR of 19 dB is required under the assumption of perfect CSI. This increases to 21 and 25 dB respectively for the cases of $\delta = 2, 0.4$. It can be noted that the slope of the curves becomes identical in

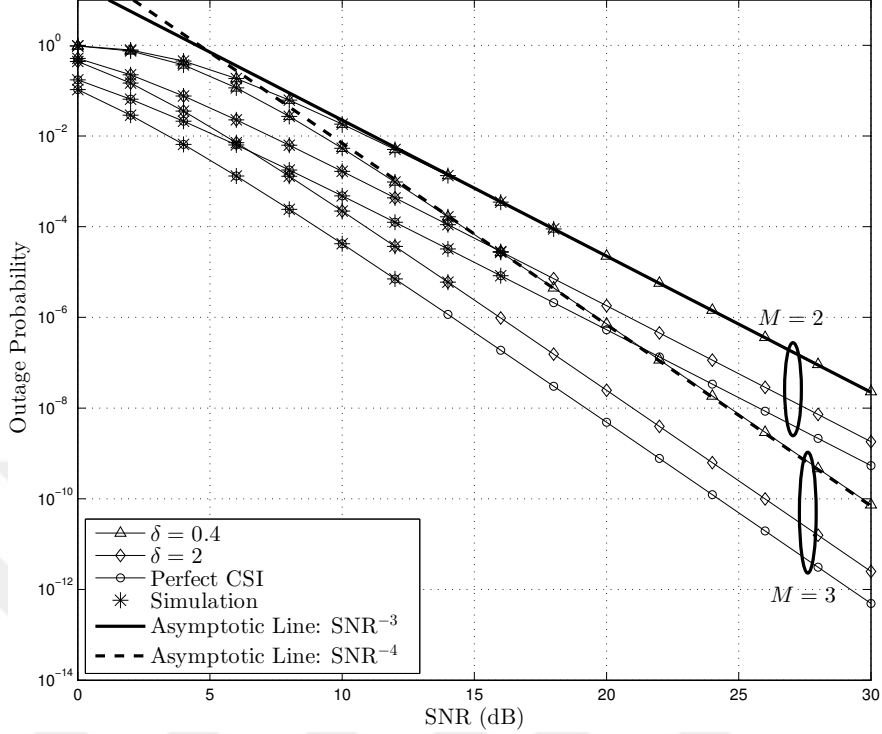


Figure 3: Outage probability of NCC system for different number of relay nodes under imperfect CSI.

high SNR regime and is equal to the maximum diversity gain $M + 1$ confirming the accuracy of (20) when $\rho \rightarrow \infty$.

Fig. 4, represents the finite-SNR diversity gain versus SNR for $P = 4$, $M = 2, 3$ and $\delta = 2$. It can be seen as SNR increases, the system can achieve higher diversity gain. In addition, NCC system with $M = 2$ and high multiplexing gain r_f has better diversity gain than that of with $M = 3$. However, as r_f decreases, higher diversity gain can be obtained for $M = 3$. More specifically, for $r_f = 0.5$, NCC system with $M = 2$ has better performance in all SNR regime. However, for lower values of multiplexing gain such as $r_f = 0.1$, the performance of the system is always better for $M = 3$. In addition, for high SNR regime, diversity gain of the system converges to its asymptotic value (22). For example at SNR=100 dB and $M = 3$ the diversity gains are 0.4, 1.89, and 3.27 for $r_f = 0.5, 0.3$ and 0.1, respectively.

Fig. 5, represents finite-SNR diversity gain versus δ for $P = 4$, $M = 2, 3$ and

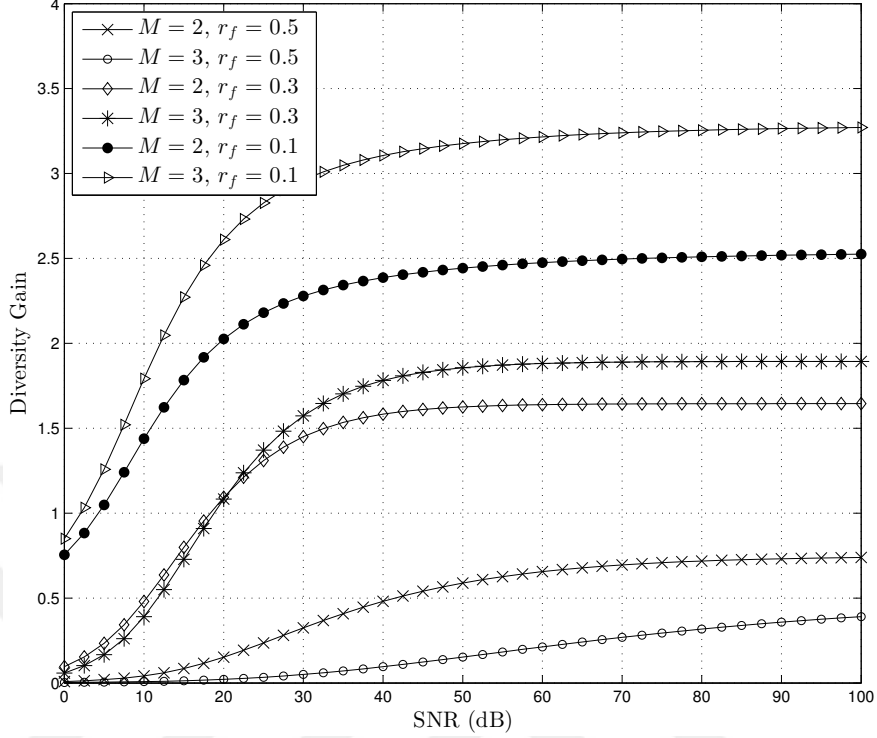


Figure 4: Finite-SNR diversity gain versus SNR.

$r_f = 0.1$. It can be seen for all values of δ , NCC system with $M = 3$ outperforms that of with $M = 2$. Furthermore, more accurate channel estimations yields higher diversity gain. However, as SNR increases, the diversity gain does not depend on the δ and is equal to (22).

Fig. 6, illustrates finite-SNR DMT curves for a system with $P = 4$, $M = 2$, $\delta = 0.4, 2$ and different values of SNR. It can be seen at practical channel estimation quality and SNR regime, the DMT of the system is significantly less than that of asymptotic one. However, by increasing SNR the DMT performance gets better and approaches to the asymptotical one given by (22). Furthermore, for the finite-SNR regime and imperfect CSI, the system cannot achieve full diversity gain of 3 at zero multiplexing gain. For example, at SNR=5 dB, the diversity gains for $\delta = 0.4, 2$ are respectively 1.94 and 1.68 while it is 1.4 for perfect CSI. These values can also be obtained by using (20) and (21) confirming the accuracy of our derivations. It

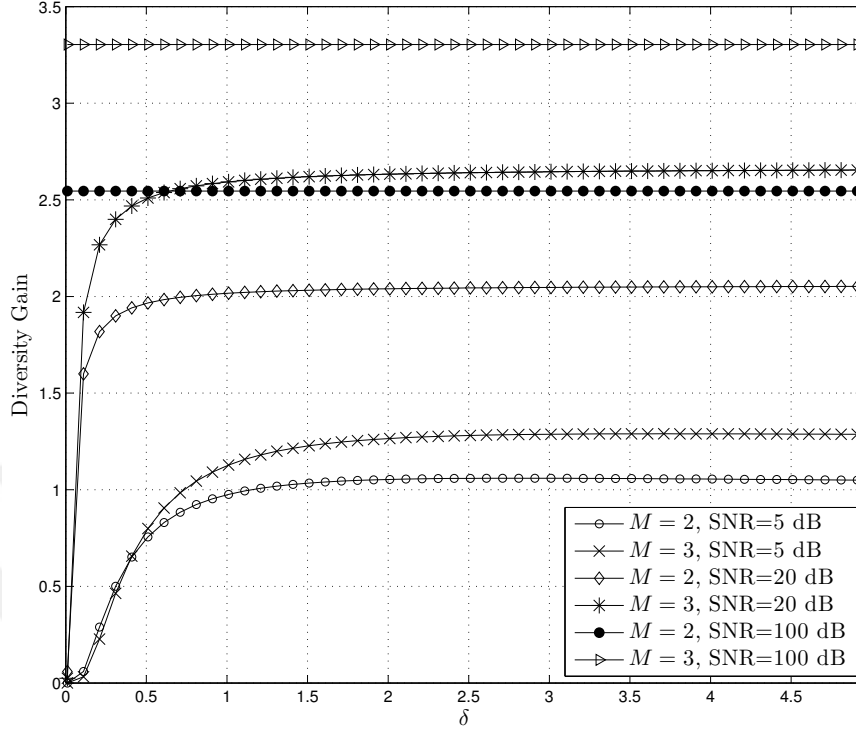


Figure 5: Finite-SNR diversity gain versus δ .

should be noted that at low values of multiplexing gain and SNR, lower values of δ i.e., worse CSI quality, achieve higher diversity gain. More specifically, for SNR=5 dB, the diversity gain for $\delta = 0.4$ is higher than that of $\delta = 2$ and perfect CSI for $r_f < 0.03$. The reason is that the error variances lead to non-zero mutual information at low multiplexing gain and low SNR regime. This leads the outage probability to decrease faster for worse channel estimation quality and therefore yields higher diversity gain. However, it can be seen that for higher values of SNR, better channel estimation quality yields higher diversity gain.

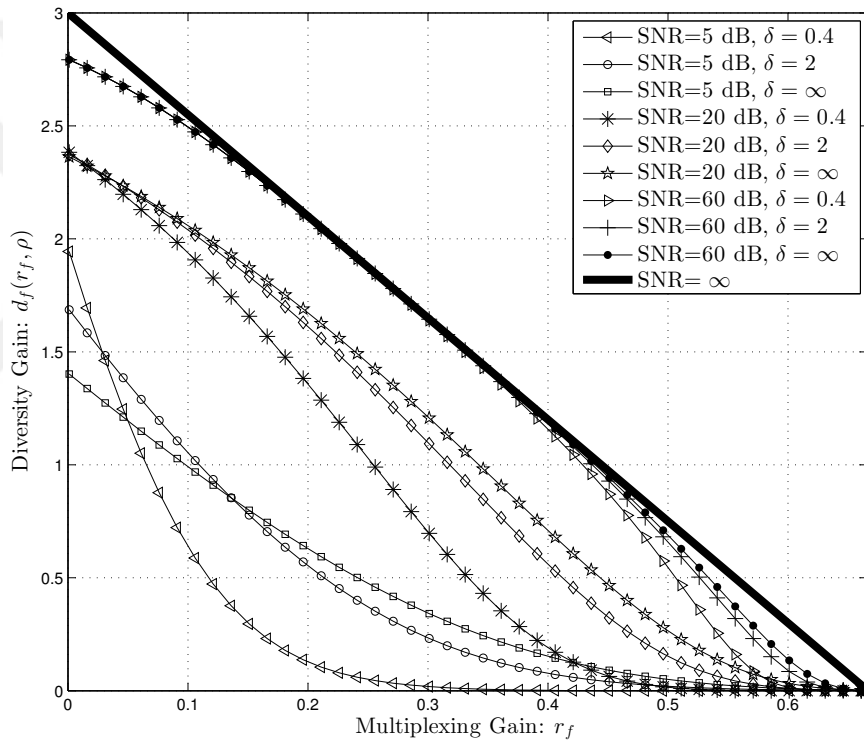


Figure 6: Finite-SNR DMT for different values of SNR under imperfect CSI.

CHAPTER III

ASYMPTOTIC DIVERSITY-MULTIPLEXING TRADEOFF FOR NETWORK CODED COOPERATIVE OFDMA SYSTEMS OVER RAYLEIGH FADING CHANNELS

In this chapter, we consider OFDMA, an extension of the OFDM to a multiuser system where subsets of carriers are assigned to different users, and investigate the outage probability and asymptotic DMT of NCC-OFDMA systems over Rayleigh fading channels. Our results demonstrate that NCC-OFDMA system is able to fully exploit both frequency and spatial diversity. Therefore NCC-OFDMA significantly outperforms stand-alone OFDMA (which only relies on frequency diversity) in terms of diversity gain. On the other hand, in NCC-OFDMA more time slots are required because of the relaying phase, therefore stand-alone OFDMA has better performance in terms of multiplexing gain. Simulation results are presented to verify our theoretical analysis.

3.1 System Model

We consider an OFDMA system with P source nodes S_i ($i = 1, \dots, P$), M relay nodes R_j ($j = 1, \dots, M$), and a single destination. We assume a total number of N subcarriers satisfying the condition of $N \geq P$, $N \geq M$. In our system, the transmission protocol consists of two phases, namely the broadcasting and the relaying phases. During the broadcasting phase, N subcarriers are allocated among P source nodes. During the relaying phase, the source nodes are silent and N subcarriers are

allocated among M relay nodes.

The destination assigns subcarriers to source and relay nodes based on the so-called maximum constraint $\kappa_{1,K}$ -matching approach (MCMA) proposed in [21]. This ensures providing the maximum number of non-outage nodes in each phase. In MCMA, the OFDMA system is modeled as a correlated random bipartite graph which consists of a set of vertices divided into two partitions such that the vertices in the same partition are not adjacent. One of these sets represents the set of users and the other represents the set of subcarriers. Subcarriers within a coherence bandwidth have highly correlated channel gains, while the channel gains of subcarriers in different coherence bandwidths are independent. An edge connects a user vertex to a subcarrier vertex if and only if the subcarrier is not in outage for a user depending on the distribution of the channel fading. Otherwise, vertices remain unconnected. After subcarrier allocation by destination using MCMA, one bit feedback per subcarrier is enough to provide information about the allocated subcarriers to each user.

Let F_i , $i = 1, \dots, P$ denote the set of subcarriers exclusively assigned to source S_i , $i = 1, \dots, P$ with $\|F_i\| = K_1 = \lfloor N/P \rfloor$ and F_j denote the set of subcarriers exclusively assigned to relay node R_j , $j = 1, \dots, M$ with $\|F_j\| = K_2 = \lfloor N/M \rfloor$.

The channel between any pair of nodes is frequency-selective quasi-static Rayleigh fading with AWGN. Let B and B_{coh} respectively denote the system bandwidth and the channel coherence bandwidth. We assume that B is large enough so that it spans L coherence bandwidths, i.e., $B = LB_{coh}$. We assume that $P > L$. The number of subcarriers within the coherence bandwidth (B_{coh}) is therefore given by $\hat{N} = N/L$.

Each packet transmitted from source node S_i consists of Q bits and is given by $I_i = (x_{i,1}[n], \dots, x_{i,w}[n])$, which is composed of w symbols drawn from a linear memoryless modulation scheme such as phase shift keying (PSK) or quadrature amplitude modulation (QAM). Here, the index n indicates that symbol is transmitted through the subcarrier $f_n \in F_{S_i}$. Similarly, each packet transmitted from each relay node has

a size of w symbols. Therefore, broadcasting and relaying phases respectively, take place over $T_1 = wT_s/K_1$ and $T_2 = wT_s/K_2$ time slots where $T_s \approx N/B$ is the symbol duration and B is the system bandwidth. This indicates that the total transmission time lasts $T_1 + T_2$ time slots. The overall transmission rate with unit in bits per second per Hertz (bits/s/Hz) is equal to

$$R = \frac{PQ}{T_2 + T_1} = \frac{PK_1K_2}{N(K_1 + K_2)}R_0, \quad (23)$$

where $R_0 = Q/w$ is transmission rate of nodes in broadcasting and relaying phases.

During broadcasting phase, each source transmits its own packet to the destination using the allocated K_1 subcarriers. OFDMA signals received by the destination and the relay nodes in the broadcasting phase are given by

$$\begin{aligned} Y_{S_iD}[n] &= \sqrt{\rho}H_{S_iD}[n]X_i[n] + W_{S_iD}[n], \\ i &= 1, \dots, P, n \in F_i \end{aligned} \quad (24)$$

$$\begin{aligned} Y_{S_iR}[n] &= \sqrt{\rho}H_{S_iR}[n]X_i[n] + W_{S_iR}[n], \\ i &= 1, \dots, P, n \in F_i \end{aligned} \quad (25)$$

where ρ is the average transmit power in each subcarrier at source node S_i , and $W_{S_iD}[n]$, $W_{S_iR}[n]$ are complex AWGN terms following $\mathcal{CN}(0, 1)$. In (24), (25), $H_{S_iD}[n]$ and $H_{S_iR}[n]$ respectively denote frequency-domain channel gains of i^{th} source-to-destination and i^{th} source-to-relay links.

In the relaying phase, relays encode the sources' packets using an encoding matrix (such as MDS codes as proposed in [10]) which describes linear relation between the sources' packets and network coding coefficients $\alpha_{i,j}$.

Each of the remaining $M - m$ relays transmits the linear combination of packets which takes the form of $I'_j = \sum_{i=1}^P \alpha_{j,i}I_i$ where $I'_j = (X'_{j,1}[n], \dots, X'_{j,w}[n])$ using

allocated K_2 subcarriers. The received signals at the destination are given by

$$Y_{R_j D}[n] = \sqrt{\rho} H_{R_j D}[n] X'_j[n] + W_{R_j D}[n], \quad n \in F_j \quad (26)$$

where $H_{R_j D}[n]$ is the frequency-domain channel gain of j^{th} relay-to-destination link, and $W_{R_j D}[n]$ is complex AWGN following $\mathcal{CN}(0, 1)$.

3.2 Derivation of Outage Probability

In this section, we first obtain outage probability per subcarrier, and then derive outage probability of the system under consideration.

3.2.1 The Outage Probability for Subcarriers

The outage probability for each subcarrier depends on the number of non-outage subcarriers that each source or relay may use. Let K_1 and K_2 respectively denote the number of non-outage subcarriers for each source and relay. In broadcasting phase, the subcarrier is in outage if it cannot support a fixed target transmission for a specific source and the corresponding outage probability is given by

$$P_{out,sub}(K_1) = \Pr \left\{ \frac{1}{N'} C_{n,i} < R_{s_1} \right\}, \quad (27)$$

where $C_{n,i}$ is instantaneous channel capacity of the link between source S_i and the destination over the subcarrier $f_n \in F_i$ and $R_{s_1} = R_0/K_1$ is the transmission rate per subcarrier. Expressing the instantaneous channel capacity as a function of SNR, (27) takes the form of

$$P_{out,sub}(K_1) = \Pr \left\{ \log_2 (1 + |H_{S_i D}[n]|^2 \rho) < R_{s_1} \hat{N} \right\}. \quad (28)$$

Since $|H_{S_i D}[n]|^2$ is exponentially distributed, we can easily obtain

$$P_{out,sub}(K_1) = \int_0^{\beta_1} \exp(-x) dx = 1 - \exp(-\beta_1), \quad (29)$$

where $\beta_1 = \left(2^{R_{s_1}\hat{N}} - 1\right) / \rho_i$. Similarly for the relaying phase, the outage probability per subcarrier for a specific relay is equal to

$$\begin{aligned} P_{out,sub}(K_2) &= \Pr \left\{ \log_2 \left(1 + |H_{R_j D}[n]|^2 \rho \right) < R_{s_2} \hat{N} \right\} \\ &= 1 - \exp(-\beta_2), \end{aligned} \quad (30)$$

where $\beta_2 = \left(2^{R_{s_2}\hat{N}} - 1\right) / \rho$ and $R_{s_2} = R_0/K_2$ is the transmission rate per subcarrier in the relaying phase.

3.2.2 The Overall Outage Probability of System

In our system, if the destination is able to decode at least P packets (either over broadcasting phase or relaying phase) from out of $P+M$ potential packets transmitted in these two phases, it is capable to recover all original packets. Due to outages in subcarriers, there may not be enough packets decoded and the overall system is in outage. The overall outage probability of the system under consideration is given by

$$P_{out} = \sum_{m=0}^M P_{out,m} P_l, \quad (31)$$

where $P_{out,m}$ denotes the probability that m out of M relays decode erroneously and P_l denotes the probability that from P source nodes and $M - m$ participating relay nodes, at most $P - 1$ nodes are not in outage. In the following, we present the calculation of each of these terms and discuss their limiting behaviors. $P_{out,m}$ can be calculated as

$$P_{out,m} = \binom{M}{m} P_R^{M-m} (1 - P_R)^m, \quad (32)$$

where P_R is the probability that any relay successfully decodes all P packets received during the broadcasting and expressed as $P_R = (1 - P_{out_1})^P$ where $P_{out_1} =$

$(P_{out,sub}(K_1))^L = (1 - \exp(-\beta_1))^L$ [21]. On the other hand, P_l is expressed as

$$P_l = \sum_{j=0}^{M-m} \binom{M-m}{j} P_{out_2}^{M-m-j} (1 - P_{out_2})^j \times \sum_{i=0}^{P-1-j} \binom{P}{i} P_{out_1}^{P-i} (1 - P_{out_1})^i, \quad (33)$$

where $P_{out_2} = (P_{out,sub}(K_2))^L = (1 - \exp(-\beta_2))^L$. Replacing (32) and (33) in (31), we have

$$P_{out} = \sum_{m=0}^M \binom{M}{m} P_R^{M-m} (1 - P_R)^m \times \sum_{j=0}^{M-m} \binom{M-m}{j} P_{out_2}^{M-m-j} (1 - P_{out_2})^j \times \sum_{i=0}^{P-1-j} \binom{P}{i} P_{out_1}^{P-i} (1 - P_{out_1})^i. \quad (34)$$

Asymptotical cases: It can be readily checked that, for asymptotically high SNR values, i.e., $\rho_i \rightarrow \infty$, we have $\beta_1 \rightarrow 0$, therefore, we obtain $\lim_{\beta_1 \rightarrow 0} P_R = 1 - PP_{out_1}$ which yields $\lim_{\beta_1 \rightarrow 0} (1 - P_R) = PP_{out_1} = P\beta_1^L$. Replacing this in (32), the first term of (31) is given by

$$\lim_{\beta_1 \rightarrow 0} \sum_{m=0}^M P_{out,m} = \sum_{m=0}^M \binom{M}{m} (P\beta_1^L)^m. \quad (35)$$

On the other hand, for $\beta_1, \beta_2 \rightarrow 0$ we have

$$\lim_{\beta_1, \beta_2 \rightarrow 0} P_l = \sum_{j=0}^{M-m} \binom{M-m}{j} \beta_2^{L(M-m-j)} \sum_{i=0}^{P-1-j} \binom{P}{i} \beta_1^{L(P-i)}. \quad (36)$$

In the high SNR regime, we can safely assume $\beta \approx \beta_1 \approx \beta_2$ and by considering the smallest order of β_1 in the second summation of (36), we obtain

$$\lim_{\beta_1, \beta_2 \rightarrow 0} P_l = \sum_{j=0}^{M-m} \binom{M-m}{j} \binom{P}{P-1-j} \beta^{L(M+1-m)}. \quad (37)$$

Finally, by substituting (35) and (37) into (34), we obtain outage probability in high SNR regime as

$$\lim_{\beta_1, \beta_2 \rightarrow 0} P_{out} = C \beta^{L(M+1)}, \quad (38)$$

where $C = \sum_{m=0}^M \binom{P+M-m}{P-1} \binom{M}{m} P^m$.

3.3 Diversity-Multiplexing Tradeoff Analysis

In this section, we first provide the DMT definition and then present the associated DMT analysis for our system. *Definition:* A scheme is said to achieve a multiplexing gain of r and a diversity gain of d , if the transmission rate satisfies [4]

$$\lim_{\rho \rightarrow \infty} \frac{R}{\log_2(\rho)} = r \quad (39)$$

and the outage probability P_{out} satisfies

$$\lim_{\rho \rightarrow \infty} \frac{\log_2(P_{out})}{\log_2(\rho)} = -d. \quad (40)$$

Theorem: The DMT of NCC-OFDMA system with P source nodes, M relays, and L coherence bandwidths using MCMA for subcarrier allocation is given by

$$d(r) = \begin{cases} L(M+1) \left(1 - \frac{P+M}{L} r\right), & r \in \left[0, \frac{L}{P+M}\right], P > M \\ L(M+1) \left(1 - \frac{M(P+M)}{PL} r\right), & r \in \left[0, \frac{PL}{M(P+M)}\right], P < M \\ L(M+1) \left(1 - \frac{2P}{L} r\right), & r \in \left[0, \frac{L}{2P}\right], P = M \end{cases} \quad (41)$$

Proof: Recall that R_{s_1} and R_{s_2} are the transmission rates per subcarrier over broadcasting and relaying phases. First consider the broadcasting phase. Substituting (23) into $R_{s_1} = R_0/K_1$, we have $R_{s_1} = N(K_1 + K_2)R / (PK_1^2 K_2)$. Replacing this expression in (38), we obtain

$$\lim_{\rho \rightarrow \infty} P_{out} = C \left(\frac{2 \frac{N^2(K_1+K_2)R}{LPK_1^2 K_2} - 1}{\rho} \right)^{L(M+1)}. \quad (42)$$

Furthermore replacing $R = r \log \rho$ in (42), we obtain

$$\lim_{\rho \rightarrow \infty} P_{out} = C \rho^{L(M+1) \left(\frac{N^2(K_1+K_2)}{LPK_1^2K_2} r - 1 \right)}. \quad (43)$$

Finally, by using the resulting expression in (40), we obtain the DMT expression

$$\begin{aligned} d(r) &= \lim_{\rho \rightarrow \infty} \frac{\log_2 \left(C \rho^{L(M+1) \left(\frac{N^2(K_1+K_2)}{LPK_1^2K_2} r - 1 \right)} \right)}{-\log_2(\rho)} \\ &= L(M+1) \left(1 - \frac{P+M}{L} r \right) \end{aligned} \quad (44)$$

where the second equality holds if $K_1 = N/P$ and $K_2 = N/M$.

The maximum diversity gain $L(M+1)$ is obtained when multiplexing gain is $r = 0$. When $d(r) = 0$, the maximum multiplexing gain $L/(P+M)$ is achieved. Therefore, the multiplexing gain r takes values between 0 and $L/(P+M)$.

Now consider the relaying phase. Substituting (23) into $R_{s_2} = R_0/K_2$, we have $R_{s_2} = N(K_1+K_2)R/(PK_1K_2^2)$. With similar steps above, the DMT expression can be obtained as

$$\begin{aligned} d(r) &= L(M+1) \left[1 - \frac{N^2(K_1+K_2)}{LPK_1K_2^2} r \right] \\ &= L(M+1) \left(1 - \frac{M(P+M)}{PL} r \right), \end{aligned} \quad (45)$$

where the multiplexing gain r takes values between 0 and $PL/(M(P+M))$.

For $P = M$, both (44) and (45) reduce to

$$d(r) = L(M+1) \left(1 - \frac{2P}{L} r \right), \quad (46)$$

where the multiplexing gain r takes values between 0 and $L/2P$.

The smaller of the maximum multiplexing gains determines the overall multiplexing gain of the system which depends on the number of source nodes and relays. When $P > M$, the maximum multiplexing gain in (44) is smaller than that of (45) i.e., $L/(P+M) < PL/(M(P+M))$, while for $P < M$ the maximum multiplexing

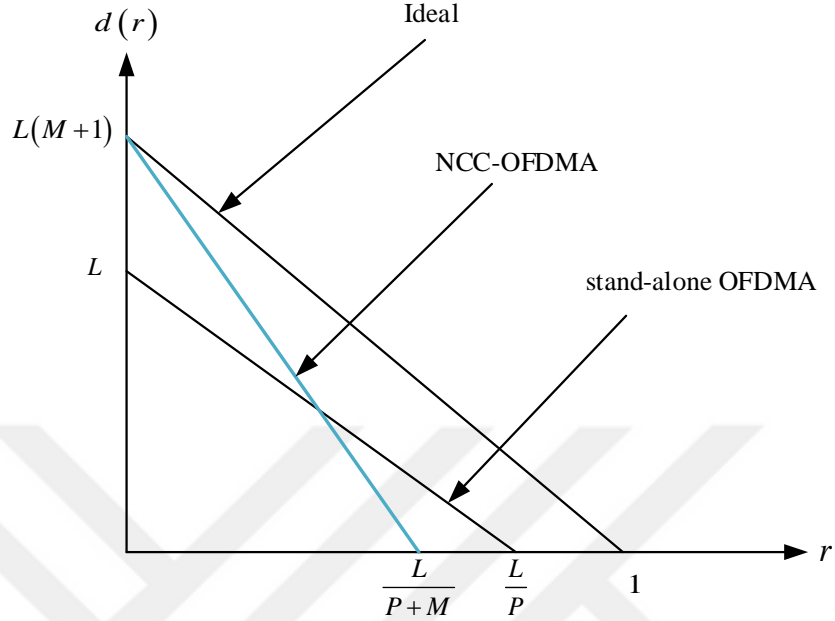


Figure 7: DMT comparison of stand-alone OFDMA and NCC-OFDMA systems ($P > M$).

gain in (45) is smaller than (44) i.e., $PL/(M(P+M)) < L/(P+M)$. Therefore, we use (44) for $P > M$ and use (45) in the case of $P < M$. Hence, we complete the proof.

Special case: If we consider that our system has no relays, i.e., $M = 0$, it can be seen from (44) that DMT equation reduces to (15) of [21] i.e., $d(r) = L(1 - rP/L)$.

Fig. 7 represents DMT curves of NCC-OFDMA and stand-alone OFDMA system [21]. In this figure, the DMT curve of (44) and that in [21] are plotted. It can be observed that the maximum diversity gain achieved by our system is equal to $L(M+1)$. This means that NCC-OFDMA is capable to exploit both frequency and spatial diversity gain and outperform stand-alone OFDMA system in terms of diversity gain. In NCC-OFDMA more time slots are required because of relaying phase, therefore stand-alone OFDMA has better performance in terms of multiplexing gain.

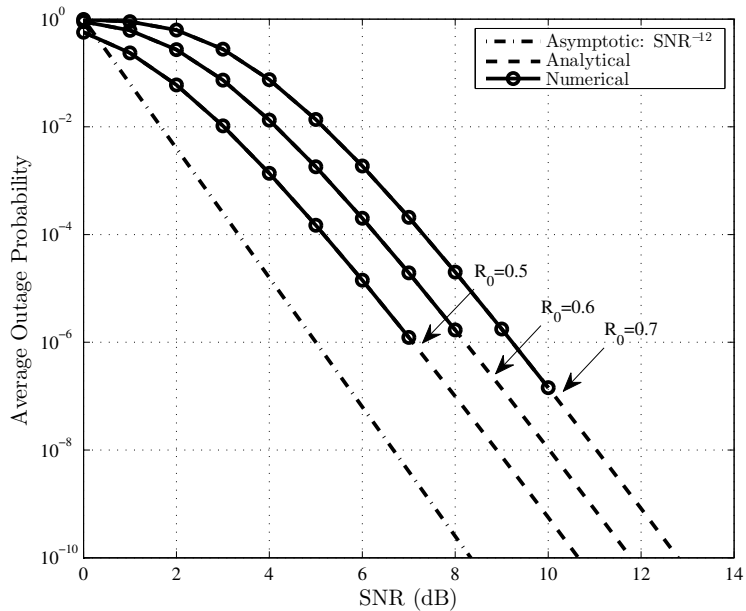


Figure 8: Outage probability for NCC-OFDMA for different values of R_0 .

3.4 Numerical Results and Discussion

In this section, we present Monte-Carlo simulations to confirm the accuracy of derived outage expression in (34). As a benchmark, the asymptotic lines $\text{SNR}^{d^*(r)2}$ are further included to verify the accuracy of diversity gains. In Monte-Carlo simulations, the channel coefficients are randomly generated following Rayleigh distribution. At each SNR, P_{out_1} and P_{out_2} are calculated to determine the outage probability in broadcasting and relaying phases, respectively. In our simulations, based on the outage state of source and relay nodes we update the rows of matrix \mathbf{Z} and determine whether the destination is capable to recover all P packets or not. If $\text{rank}(\mathbf{Z}) < P$, we declare that the system is in outage, otherwise it is capable to recover all original packets $I_i (i = 1, \dots, P)$.

In Fig. (8), we assume that the number of coherence bandwidths is $L = 4$, the number of subcarriers is $N = 128$, the number of source nodes is $P = 8$, and the number of relays is $M = 2$ and present the exact outage probability of NCC-OFDMA for different transmission rates $R_0 = 0.5, 0.6, 0.7$ along with Monte-Carlo simulation

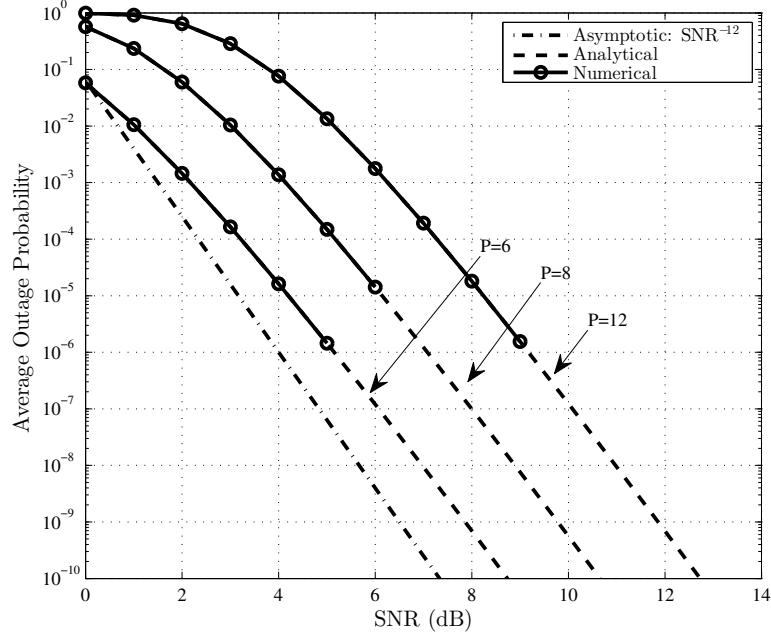


Figure 9: Outage probability of NCC-OFDMA for different values of P .

results. It is observed that the derived expression in (34) is in excellent agreement with simulation results. It is also observed that as R_0 increases, the system is more likely to undergo outage, leading higher values of outage. For example, at $R_0 = 0.5$, SNR of 5 dB is required to achieve an outage probability of 10^{-4} . This climbs to 6 dB and 7 dB, respectively for $R_0 = 0.6$ and $R_0 = 0.7$. However the slopes of the curves remain constant and all of them provide a diversity gain of $L(M + 1) = 12$ confirming the derived maximum diversity gain as observed from (41).

In Fig. (9), we assume $L = 4$, $N = 128$, $M = 2$, and $R_0 = 0.5$ and present the outage performance for different number of source nodes i.e., for $P = 6, 8, 12$. Similar to Fig. 12, the derived exact expression perfectly matches to simulation results. It is also observed that when the number of source nodes increases, the system performance deteriorates. For example, for the system with $P = 6$ sources, an outage probability of 10^{-6} is achieved at SNR=5 dB. For the same SNR values, the systems with $P = 8$ and $P = 12$ sources are able to achieve outage probability of 10^{-4} and 10^{-2} , respectively. However, due to the fact that diversity gain does not depend on the number of sources,

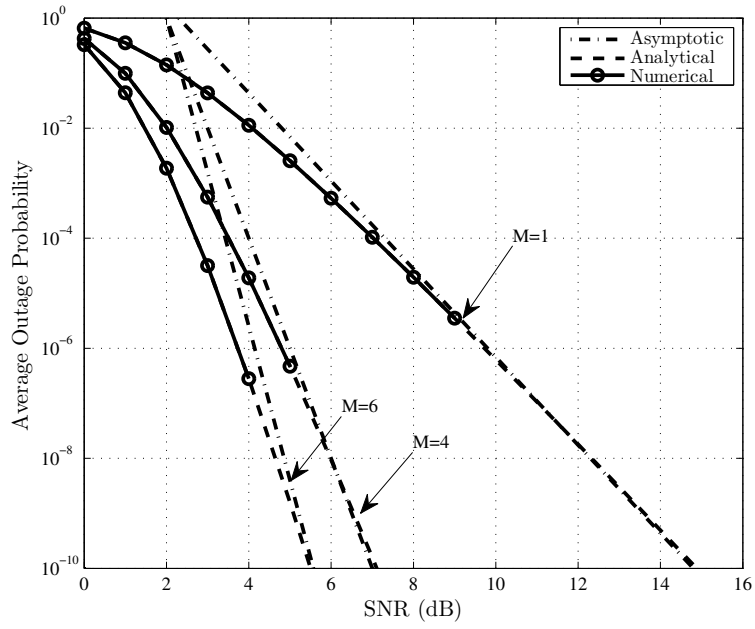


Figure 10: Outage probability of NCC-OFDMA for different values of M .

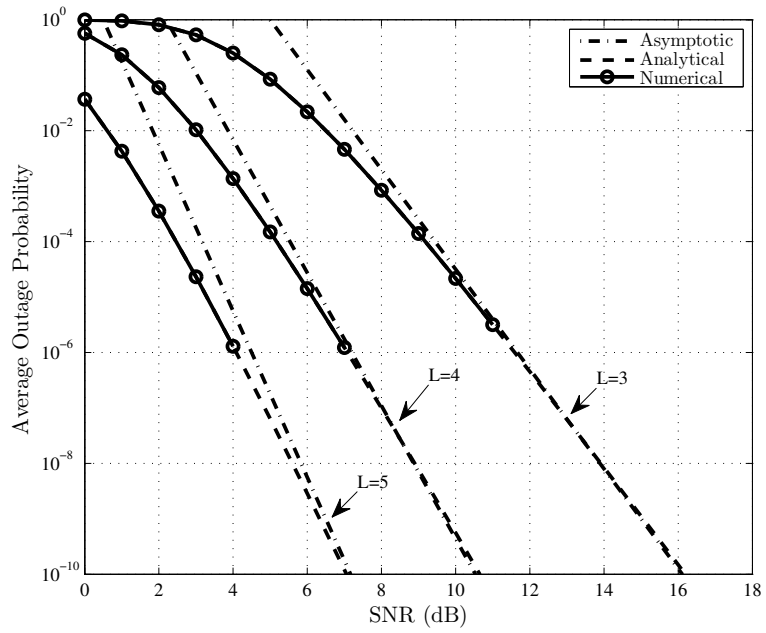


Figure 11: Outage probability for NCC-OFDMA for different values of L .

as observed from (41), all systems yield a diversity gain of 12.

In Fig. 10, we assume $L = 4$, $N = 128$, $P = 8$, and $R_0 = 0.5$ and present the outage performance for different number of relays, i.e., $M = 1, 4, 6$. When $M = 1$, SNR of 15 dB is required to achieve an outage probability of 10^{-10} . This decreases to about 7 dB and 5 dB, respectively for $M = 4$ and $M = 6$. It is also observed that having more relays offers more diversity gain for a given R_0 . The diversity gain for $M = 1$ is equal to 8 while for $M = 4$ and $M = 6$ respectively, are 20 and 28.

In Fig. 11, we assume $N = 128$, $P = 8$, $M = 2$, and $R_0 = 0.5$ and present the outage performance for $L = 3, 4, 5$. Recall that L is the ratio of between system bandwidth and coherence bandwidth. It is observed that the increase in L results in the increase of diversity gain. The diversity gains achieved for $L = 3, 4, 5$ are respectively, 9, 12, and 15.

CHAPTER IV

FINITE-SNR DIVERSITY-MULTIPLEXING TRADEOFF FOR NETWORK CODED COOPERATIVE OFDMA SYSTEMS OVER RICIAN FADING CHANNELS

In this chapter, we derive an exact closed-form outage probability of NCC-OFDMA systems over Rician fading channels and obtain asymptotical DMT expression. Asymptotical DMT of Rician fading channels coincides with that of Rayleigh channel and does not provide insight into practical SNR ranges. We further derive finite-SNR DMT over Rician fading channels. As opposed to Rayleigh fading, for Rician fading, the maximum diversity gain does not always occur at zero multiplexing gain. It can be observed from our results that the presence of LOS components in Rician fading leads diversity gains higher than asymptotic SNR values at some SNRs and multiplexing gains. We also demonstrate that finite-DMT expression is equivalent to the conventional DMT expression when SNR approaches to its asymptotic value.

4.1 *System Model*

We consider the same NCC-OFDMA system model as explained in chapter 3. We assume that the channel between any pair of nodes is identically independent frequency-selective quasi-static Rician fading. Let $H_{XY}[n]$, $XY \in \{S_iD, S_iR, R_jD\}$ denotes the frequency domain channel gain of $X \rightarrow Y$ link at subcarrier n . The envelope of $H_{XY}[n]$ follows Rician distribution [35]. $H_{XY}[n]$ can be expressed as

$$H_{XY}[n] = \sqrt{\frac{k}{k+1}} + \sqrt{\frac{1}{k+1}} \tilde{H}_{XY}[n], \quad (47)$$

where $k \geq 0$ is the Rician factor defined as the power ratio between the LOS and random (scattered) components. In (47), $\tilde{H}_{XY}[n]$ is complex Gaussian random variable with unit average power and modeled as $\tilde{H}_{XY}[n] = \sqrt{0.5}(a + jb)$, where a and b are circularly symmetric Gaussian distributed random variables with variance one. It can be noted that the envelope of $\tilde{H}_{XY}[n]$ is Rayleigh distributed and for $k = 0$ $H_{XY}[n] = \tilde{H}_{XY}[n]$.

In following, we first obtain outage probability per subcarrier over Rician fading channels and then derive outage probability of the overall system.

4.2 Derivation of Outage Probability

4.2.1 Outage Probability for Subcarriers

In broadcasting phase, the subcarrier is in outage if it cannot support a fixed target transmission rate for a specific source. Since $H_{XY}[n]$ is complex Gaussian distributed with non-zero mean, $|H_{XY}[n]|^2$ is non-central chi-square distributed with two degrees of freedom. The cumulative distribution function (CDF) of $|H_{S_iD}[n]|^2$ is given by

$$F_{|H_{S_iD}[n]|^2}(y) = 1 - Q_1\left(\sqrt{2k}, \sqrt{2(1+k)y}\right). \quad (48)$$

Using (28), we have

$$P_{out_{sub}'}(K_1) = 1 - Q_1(\alpha, \beta_1), \quad (49)$$

where $\alpha = \sqrt{2k}$ and $\beta_1 = \sqrt{2(1+k)(2^{R_{s_1}\hat{N}} - 1)}/\rho$. Similarly, for $S_i \rightarrow R$ link, the outage probability of the subcarriers can be obtained and has a similar form of (48).

For the relaying phase i.e., $R_j \rightarrow D$, the outage probability per subcarrier for a specific relay is equal to

$$\begin{aligned} P_{out_{sub}'}(K_2) &= \Pr\left\{\log_2\left(1 + |H_{R_jD}[n]|^2\rho\right) < R_{s_2}\hat{N}\right\} \\ &= 1 - Q_1(\alpha, \beta_2), \end{aligned} \quad (50)$$

where $\beta_2 = \sqrt{2(1+k)(2^{R_{s_2}\hat{N}} - 1)}/\rho$.

4.2.2 Overall Outage Probability

Substituting (49) and (50) in (34), we have

$$\begin{aligned}
P_{out}(R_0, \rho) &= \sum_{m=0}^M \binom{M}{m} P_R^{M-m} (1 - P_R)^m \\
&\times \sum_{j=0}^{M-m} \binom{M-m}{j} P_{outRD}^{M-m-j} (1 - P_{outRD})^j \\
&\times \sum_{i=0}^{P-1-j} \binom{P}{i} P_{outSD}^{P-i} (1 - P_{outSD})^i.
\end{aligned} \tag{51}$$

In (51), $P_R = (1 - P_{outSR})^P$ where $P_{outSR} = (P_{out_{sub'}}(K_1))^L = (1 - Q_1(\alpha, \beta_1))^L$ [21] is the outage probability of the link $S \rightarrow R$. $P_{outRD} = ((P_{out_{sub'}}(K_2))^L = (1 - Q_1(\alpha, \beta_2))^L$, $P_{outSD} = ((P_{out_{sub'}}(K_1))^L = (1 - Q_1(\alpha, \beta_1))^L$ respectively denote the outage probability of the link $R \rightarrow D$ and $S \rightarrow D$.

4.3 DMT Analysis

4.3.1 Derivation of Asymptotical DMT

Recall that the variables $\alpha = \sqrt{2k}$ and $\beta_1 = \sqrt{2(1+k)(2^{R_{s1}\hat{N}} - 1)}/\rho$ in (48) are Rician factor (k) dependent. It can be readily checked that for asymptotically high SNR values, i.e., $\rho \rightarrow \infty$, we have $\beta_1 \rightarrow 0$ and therefore $P_{outSR} \rightarrow 0$ which yields $\lim_{\beta_1 \rightarrow 0} P_R = 1 - P P_{outSR}$. Thus, $\lim_{\beta_1 \rightarrow 0} (1 - P_R) = \lim_{\beta_1 \rightarrow 0} P (1 - Q_1(\alpha, \beta_1))^L$. Marcum Q -function is given in terms of its series form as [36]

$$Q_1(\alpha, \beta) = 1 - \exp\left(-\frac{\alpha^2 + \beta^2}{2}\right) \sum_{m=1}^{\infty} \left(\frac{\beta}{\alpha}\right)^m I_m(\alpha\beta). \tag{52}$$

In (52), we use the power series expansion for modified Bessel function [37] and replace exponential function with its Maclaurin series form [38] to find the smallest order of β_1 . This results in $\lim_{\beta_1 \rightarrow 0} Q_1(\alpha, \beta_1) = 1 - \exp(-\alpha^2/2) \beta_1^2/2$. Therefore, we have

$$\lim_{\beta_1 \rightarrow 0} (1 - P_R) = P \left(\exp\left(-\frac{\alpha^2}{2}\right) \frac{\beta_1^2}{2} \right)^L. \tag{53}$$

After some mathematical manipulation as we did in chapter 3, we finally have

$$\lim_{\beta \rightarrow 0} P_{out}(R_0, \rho) = C \left(\exp\left(-\frac{\alpha^2}{2}\right) \frac{\beta^2}{2} \right)^{L(M+1)}, \quad (54)$$

where $C = \sum_{m=0}^M \binom{P+M-m}{P-1} \binom{M}{m} P^m$.

Theorem: The asymptotic DMT of NCC-OFDMA system over Rician fading channel with P source nodes, M relay nodes, and L coherence bandwidths using MCMA for subcarrier allocation is given by

$$d(r) = \begin{cases} L(M+1) \left(1 - \frac{P+M}{L}r\right), & r \in \left[0, \frac{L}{P+M}\right], P > M \\ L(M+1) \left(1 - \frac{M(P+M)}{PL}r\right), & r \in \left[0, \frac{PL}{M(P+M)}\right], P < M \\ L(M+1) \left(1 - \frac{2P}{L}r\right), & r \in \left[0, \frac{L}{2P}\right], P = M \end{cases} \quad (55)$$

Proof: Recall that R_{s_1} and R_{s_2} are the transmission rates per subcarrier over broadcasting, and relaying phases. Substituting (23) into $R_{s_1} = R_0/K_1$, we have $R_{s_1} = N(K_1 + K_2)R/(PK_1^2K_2)$. Replacing this expression in (54), we obtain

$$\lim_{\rho \rightarrow \infty} P_{out} = \xi \left(\frac{2 \frac{N^2(K_1+K_2)R}{LPK_1^2K_2} - 1}{\rho} \right)^{L(M+1)}, \quad (56)$$

where $\xi = C \exp(-L(M+1)\alpha^2/2)(1+k)^{L(M+1)}$. Following same steps as we did in chapter 3, we obtain (55).

Special case I: It should be noted that due to the dominant scattered component in high SNR regime, the slopes of the outage probability in the case of Rician fading channel and Rayleigh fading channel ($k = 0$) are identical. Therefore, the asymptotical DMT expression in (55) derived for Rician fading coincides to that of Rayleigh fading (41).

4.3.2 Derivation of Finite-SNR DMT

We have $R(\rho) = r_f \log_2(1 + \rho)$ [22]. Substituting it into β_1 and β_2 , we respectively have

$$\bar{\beta}_1 = \sqrt{2(1+k) \left((1+\rho)^{(P+M)r_f/L} - 1 \right)} / \rho, \quad (57)$$

and

$$\bar{\beta}_2 = \sqrt{2(1+k) \left((1+\rho)^{M(P+M)r_f/(PL)} - 1 \right)} / \rho. \quad (58)$$

Inserting (57) and (58) into (51), we can express the outage probability in terms of r_f and ρ as

$$\begin{aligned} P_{out}(r_f, \rho) &= \sum_{m=0}^M \binom{M}{m} \bar{P}_R^{M-m} (1 - \bar{P}_R)^m \\ &\times \sum_{j=0}^{M-m} \binom{M-m}{j} \bar{P}_{outRD}^{M-m-j} (1 - \bar{P}_{outRD})^j \\ &\times \sum_{i=0}^{P-1-j} \binom{P}{i} \bar{P}_{outSD}^{P-i} (1 - \bar{P}_{outSD})^i, \end{aligned} \quad (59)$$

where $\bar{P}_R = \left(1 - (1 - Q_1(\alpha, \bar{\beta}_1))^L\right)^P$, $\bar{P}_{outRD} = (1 - Q_1(\alpha, \bar{\beta}_2))^L$, and $\bar{P}_{outSD} = (1 - Q_1(\alpha, \bar{\beta}_1))^L$.

Noting that $\partial Q_1(\alpha, \beta) / \partial \beta = -\beta \exp(-(\alpha^2 + \beta^2)/2) I_0(\alpha\beta)$ and after some mathematical manipulations in (59), the finite-SNR DMT is given by

$$\begin{aligned} d_f(r_f, \rho) &= -\frac{\rho}{P_{out}(r_f, \rho)} \frac{\partial P_{out}(r_f, \rho)}{\partial \rho} \\ &= \frac{\zeta_1 + \zeta_2 + \zeta_3}{P_{out}(r_f, \rho)}, \end{aligned} \quad (60)$$

where ζ_1 , ζ_2 , and ζ_3 are respectively defined as

$$\begin{aligned}
\zeta_1 &= \sum_{m=0}^M \binom{M}{m} \Omega(\bar{\beta}_1) \Lambda(L) P (1 - \bar{P}_{outSR})^{P-1} \\
&\times (1 - \bar{P}_R)^{m-1} \bar{P}_R^{M-m-1} L (m - M (1 - \bar{P}_R)) \\
&\times \sum_{j=0}^{M-m} \binom{M-m}{j} \bar{P}_{outRD}^{M-m-j} (1 - \bar{P}_{outRD})^j \\
&\times \sum_{i=0}^{P-1-j} \binom{P}{i} \bar{P}_{outSD}^{P-i} (1 - \bar{P}_{outSD})^i, \tag{61}
\end{aligned}$$

$$\begin{aligned}
\zeta_2 &= \sum_{j=0}^{M-m} \binom{M-m}{j} \Omega(\bar{\beta}_2) \Lambda\left(\frac{PL}{M}\right) (1 - \bar{P}_{outRD})^{j-1} \\
&\times \bar{P}_{outRD}^{M-m-j-1} L (M - m - j - (M - m) \bar{P}_{outRD}) \\
&\times \sum_{m=0}^M \binom{M}{m} \bar{P}_R^{M-m} (1 - \bar{P}_R)^m \\
&\times \sum_{i=0}^{P-1-j} \binom{P}{i} \bar{P}_{outSD}^{P-i} (1 - \bar{P}_{outSD})^i, \tag{62}
\end{aligned}$$

$$\begin{aligned}
\zeta_3 &= \sum_{i=0}^{P-1-j} \binom{P}{i} \Omega(\bar{\beta}_1) \Lambda(L) (1 - \bar{P}_{outSD})^{i-1} \bar{P}_{outSD}^{P-i-1} \\
&\times L (P - i - P \bar{P}_{outSD}) \sum_{m=0}^M \binom{M}{m} \bar{P}_R^{M-m} (1 - \bar{P}_R)^m \\
&\times \sum_{j=0}^{M-m} \binom{M-m}{j} \bar{P}_{outRD}^{M-m-j} (1 - \bar{P}_{outRD})^j. \tag{63}
\end{aligned}$$

In (61)-(63), $\Omega(\cdot)$ and $\Lambda(\cdot)$ are respectively expressed as

$$\Omega(\omega) = (1 - Q_1(\alpha, \omega))^{L-1} \exp\left(-\frac{\alpha^2 + \omega^2}{2}\right) \left(\frac{\omega^2}{2}\right) I_0(\alpha\omega) \tag{64}$$

and

$$\Lambda(\lambda) = 1 - \frac{\frac{(P+M)}{\lambda} r_f \rho (1 + \rho)^{\frac{(P+M)}{\lambda} r_f - 1}}{(1 + \rho)^{\frac{(P+M)}{\lambda} r_f} - 1}. \quad (65)$$

4.3.3 Asymptotic Behavior of Finite-SNR DMT

In this section, we demonstrate that asymptotical DMT can be obtained as a special case of the finite-SNR DMT. It can be readily checked that, for asymptotically high SNR values, we have $\lim_{\rho \rightarrow \infty} \bar{\beta}_1 = \sqrt{2(1+k)} \rho^{((P+M)r/L)-1}$ and $\lim_{\rho \rightarrow \infty} \bar{\beta}_2 = \sqrt{2(1+k)} \rho^{(M(P+M)r/(PL))-1}$. From (41) we have $r < \min(L/(P+M), PL/(M(P+M)))$, therefore $\bar{\beta} \approx \lim_{\rho \rightarrow \infty} \bar{\beta}_1 \approx \lim_{\rho \rightarrow \infty} \bar{\beta}_2 \approx 0$. Following the same steps as in section 4.3.2 we obtain

$$\lim_{\bar{\beta} \rightarrow \infty} P_{out}(r_f, \rho) = C \left(\exp\left(-\frac{\alpha^2}{2}\right) \frac{\bar{\beta}^2}{2} \right)^{L(M+1)}. \quad (66)$$

Now consider $\lim_{\rho \rightarrow \infty} -\rho \partial P_{out}(r, \rho) / \partial \rho$. By Noting that $\lim_{\omega \rightarrow 0} \Omega(\omega) = (\exp(-\alpha^2/2) \omega^2/2)^L$, and $\lim_{\rho \rightarrow \infty} \Lambda(\lambda) = 1 - (P+M)r/\lambda$, we have

$$\lim_{\bar{\beta}_1 \rightarrow 0} \zeta_1 = C \left(\exp\left(\frac{\alpha^2}{2}\right) \frac{\bar{\beta}_1^2}{2} \right)^{L(M+1)} \left(1 - \frac{P+M}{L} r\right) Lm, \quad (67)$$

$$\lim_{\bar{\beta}_2 \rightarrow 0} \zeta_2 = C \left(\exp\left(\frac{\alpha^2}{2}\right) \frac{\bar{\beta}_2^2}{2} \right)^{L(M+1)} \left(1 - \frac{M(P+M)}{PL} r\right) L(M-m-j), \quad (68)$$

and

$$\lim_{\bar{\beta}_1 \rightarrow 0} \zeta_3 = C \left(\exp\left(\frac{\alpha^2}{2}\right) \frac{\bar{\beta}_1^2}{2} \right)^{L(M+1)} \left(1 - \frac{P+M}{L} r\right) L(j+1). \quad (69)$$

For the case of $P > M$, maximum multiplexing gain is limited by $L/(P+M)$. Hence, we replace the term $1 - (M(P+M))r/(PL)$ of (68) by $1 - (P+M)r/L$. Therefore, we obtain

$$\begin{aligned} \lim_{\bar{\beta} \rightarrow 0} \frac{-\rho \partial P_{out}(r_f, \rho)}{\partial \rho} &= \lim_{\bar{\beta}_1 \rightarrow 0} \zeta_1 + \lim_{\bar{\beta}_2 \rightarrow 0} \zeta_2 + \lim_{\bar{\beta}_1 \rightarrow 0} \zeta_3 \\ &= C \left(\exp\left(\frac{\alpha^2}{2}\right) \frac{\bar{\beta}^2}{2} \right)^{L(M+1)} L(M+1) \left(1 - \frac{P+M}{L} r\right). \end{aligned} \quad (70)$$

Finally, by substituting (66) and (70) into (7), we obtain

$$\lim_{\rho \rightarrow \infty} d_f(r_f, \rho) = L(M+1) \left(1 - \frac{P+M}{L} r \right). \quad (71)$$

With similar steps above, we can obtain DMT relations in asymptotic case for $P < M$ and $P = M$. For the case of $P < M$, the maximum multiplexing gain is limited by $PL/(M(P+M))$, therefore, we replace the term $1 - (P+M)r/L$ of (67) and (69) by $1 - (M(P+M))r/(PL)$. For $P = M$, both $1 - (P+M)r/L$, and $1 - (M(P+M))r/(PL)$ reduce to $1 - 2Pr/L$. This demonstrates that the derived finite-SNR DMT in Section 4.3.3 converges to the asymptotical one presented in Section 4.3.2 as expected confirming the accuracy of our derivations.

4.3.4 Finite-SNR Diversity Gain for a Fixed transmission Rate

Here, we investigate finite-SNR diversity gain where transmission rate R_0 is fixed. By substituting (51) into (7) and after some mathematical manipulations, we have

$$\begin{aligned} d_f(R_0, \rho) &= -\frac{\rho}{P_{out}(R_0, \rho)} \frac{\partial P_{out}(R_0, \rho)}{\partial \rho} \\ &= \frac{\zeta'_1 + \zeta'_2 + \zeta'_3}{P_{out}(R_0, \rho)}, \end{aligned} \quad (72)$$

where ζ'_1 , ζ'_2 , and ζ'_3 are respectively expressed as

$$\begin{aligned} \zeta'_1 &= \sum_{m=0}^M \binom{M}{m} \Omega(\beta_1) P (1 - P_{out_{SR}})^{P-1} (1 - P_R)^{m-1} \\ &\quad \times P_R^{M-m-1} L(m - M(1 - P_R)) \\ &\quad \times \sum_{j=0}^{M-m} \binom{M-m}{j} P_{out_{RD}}^{M-m-j} (1 - P_{out_{RD}})^j \\ &\quad \times \sum_{i=0}^{P-1-j} \binom{P}{i} P_{out_{SD}}^{P-i} (1 - P_{out_{SD}})^i, \end{aligned} \quad (73)$$

$$\begin{aligned}
\zeta_2' &= \sum_{j=0}^{M-m} \binom{M-m}{j} \Omega(\beta_2) (1 - P_{outRD})^{j-1} \\
&\times P_{outRD}^{M-m-j-1} L(M-m-j - (M-m) P_{outRD}) \\
&\times \sum_{m=0}^M \binom{M}{m} P_R^{M-m} (1 - P_R)^m \\
&\times \sum_{i=0}^{P-1-j} \binom{P}{i} P_{outSD}^{P-i} (1 - P_{outSD})^i, \tag{74}
\end{aligned}$$

$$\begin{aligned}
\zeta_3' &= \sum_{i=0}^{P-1-j} \binom{P}{i} \Omega(\beta_1) (1 - P_{outSD})^{i-1} P_{outSD}^{P-i-1} \\
&\times L(P-i - P P_{outSD}) \\
&\times \sum_{m=0}^M \binom{M}{m} P_R^{M-m} (1 - P_R)^m \\
&\times \sum_{j=0}^{M-m} \binom{M-m}{j} P_{outRD}^{M-m-j} (1 - P_{outRD})^j. \tag{75}
\end{aligned}$$

From (60) and (72), it can be easily checked that $d(r_f, \rho) = \Lambda(L) (\zeta_1' + \zeta_3')|_{R=r_f \log_2(1+\rho)} + \Lambda(PL/M) \zeta_2'|_{R=r_f \log_2(1+\rho)}$. When $\rho \rightarrow \infty$, we obtain

$$\lim_{\rho \rightarrow \infty} d_f(R_0, \rho) = L(M+1). \tag{76}$$

It is expected that in high SNR regime the diversity gain at the fixed R_0 (72) becomes equal to $\lim_{\rho \rightarrow \infty} d_f(r_f, \rho)|_{r=0}$ or equivalently equal to (55) when $r = 0$. It can be easily checked that for $r = 0$, (55) yields $L(M+1)$ which is consistent with (76). This result indicates that in high SNR regime the diversity gain of system is restricted by the number of relay nodes and number of coherence bandwidths.

Special Case II: For Rayleigh fading channels, we have $k = 0$, hence the Marcum Q -function in (49) is reduced to exponential function [36]. Then, we can obtain the

finite-SNR DMT and diversity gain for Rayleigh fading channels. The associated analytical results are provided in the following section.

4.4 Numerical Results and Discussion

In this section, we present analytical results as well as Monte-Carlo simulations to confirm the accuracy of our derivations. As a benchmark, we also plot curves for $k = 0$ i.e., the channel gains follow Rayleigh distribution.

Fig. 12 demonstrates the outage probability given by (51) along with the Monte-Carlo simulation results for $N = 128$ subcarriers, $P = 4$ source nodes, $M = 1, 2$ relay nodes assuming a transmission rate of $R_0 = 0.5$, Rician factor $k = 6, 8$ dB and $L = 2$ coherence bandwidths. It is observed that the derived expression in (51) is in excellent agreement with simulation results confirming the accuracy of our derivation. It is also observed that an impressive performance improvement is obtained through spatial diversity gain achieved by relay nodes. Specially, the required SNR to achieve a target outage probability of 10^{-6} for non-cooperative case ($M = 0$) i.e., stand-alone OFDMA system is 16 dB over a Rician channel with $k = 8$ dB. This reduces to 7.8 dB for $M = 1$. It further reduces to 5.5 dB for $M = 2$. It should be noted that we plot the analytical curves for extremely low values up to 10^{-30} to clearly observe the slope of the curves in high SNR regime. It can be seen that the slope of the plots are identical to that of asymptotic lines. The diversity gains in high SNR regime for $M = 1, 2$ are respectively equal to 4 and 6 confirming that the diversity gain is determined by $L(M + 1)$. As expected, due to the dominant of the scattered component in high SNR regime, the slope of the outage probability over Rician fading channel is identical to that of Rayleigh fading channel ($k = 0$).

Fig. 13 depicts finite diversity gain, i.e., $d_f(R_0, \rho)$ at a fixed transmission rate given by (72). We consider the same parameters as in Fig. 12. As can be seen in Fig. 12, in finite-SNR regime there is a significant drop in the outage probability

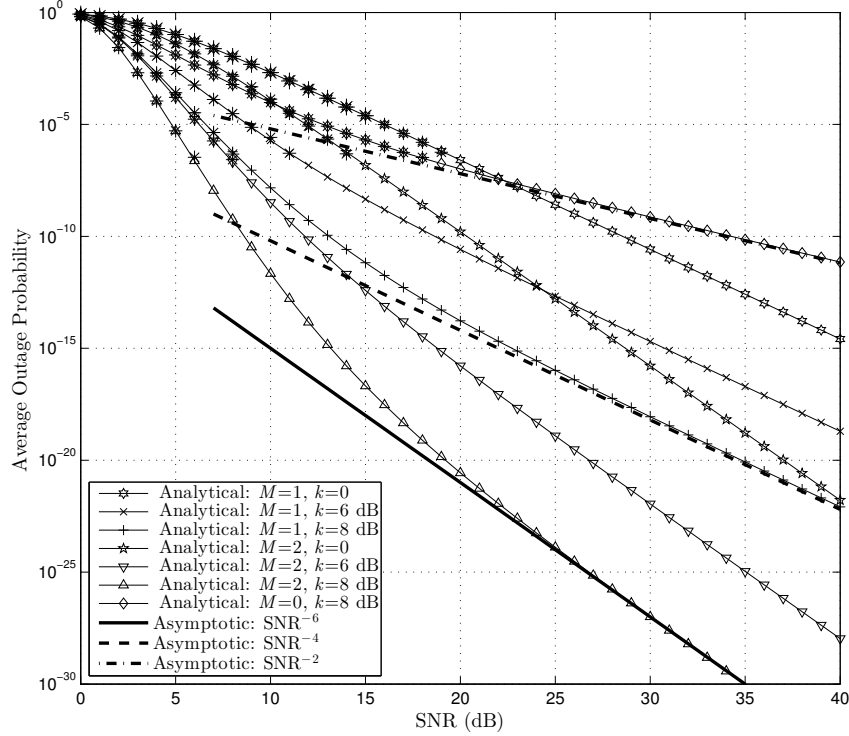


Figure 12: Outage probability for different values of M .

which leads to have a peak in the finite-SNR diversity gain as shown in Fig. 13. Specifically, the maximum diversity gain is achieved at $\text{SNR}=5$ dB for $M = 1, 2$. As the Rician factor increases, higher diversity gains are obtained. This is due to the presence of LOS in finite-SNR regime playing as an additional diversity source. For higher values of SNR, the scattered component begins to dominate the performance of the system and therefore decreases the diversity gain to $L(M + 1)$ given by (76). It should be further emphasized that, in contrast to Rician fading channels, there is not such a diversity peak in finite SNR regime for Rayleigh fading channels. The maximum diversity gain is achieved at asymptotically high SNR values and is equal to that of Rician channels.

Fig. 14 presents finite diversity gain versus SNR for various number of coherence bandwidths $L = 2, 3$ assuming $N = 128$, $P = 4$, $M = 1$, $R_0 = 0.5$, and $k = 6$ dB. It can be seen that for the high SNR regime the diversity gain for $L = 2, 3$ are

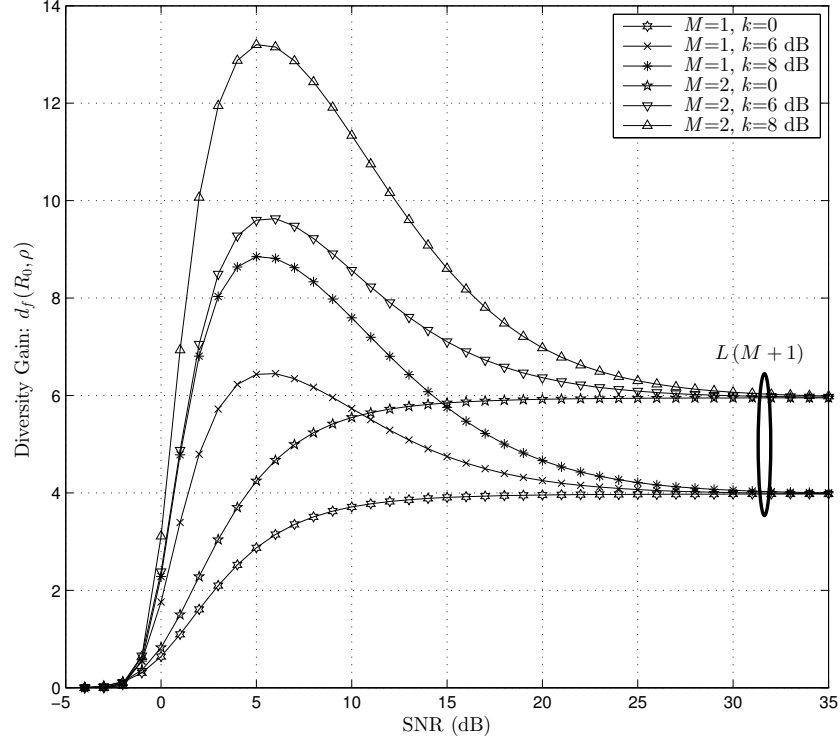


Figure 13: Diversity gain for different values of M at fixed transmission rate.

respectively 4 and 6 confirming (76).

In Fig. 15, we assume $L = 2$, $N = 128$, $P = 4$, $M = 1$, $k = 6$ dB, and investigate the diversity gain for various values of $R_0 = 0.5, 0.7, 1$. As can be seen from figure, the asymptotic diversity gains are independent of R_0 and do not change. This indicates that diversity gain does not depend on transmission rate and just by increasing R_0 the system is more likely to undergo outage, leading higher values of outage.

In Fig. 16, we assume $L = 2$, $N = 128$, $M = 1$, $k = 6$ dB, and $R_0 = 0.5$ and investigate the diversity gain for various values of $P = 4, 8, 12$. It is obvious that by increasing the number of source nodes the outage probability of the system increases. However, the asymptotic diversity gain of the system does not change. It is observed that for all different values of P the diversity gain of the system in high SNR regime is equal to 4.

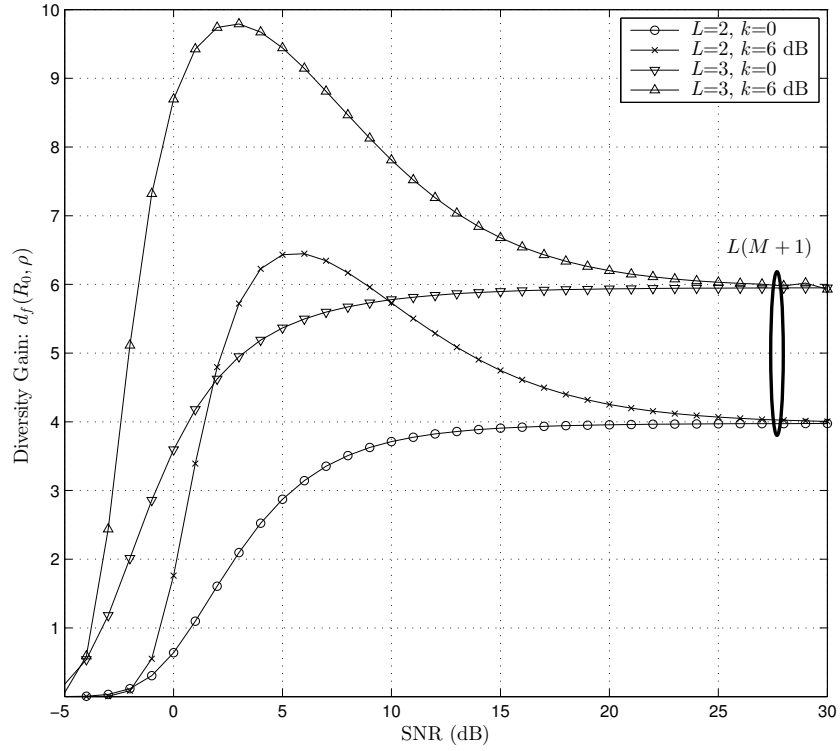


Figure 14: Diversity gain for different values of L at fixed transmission rate.

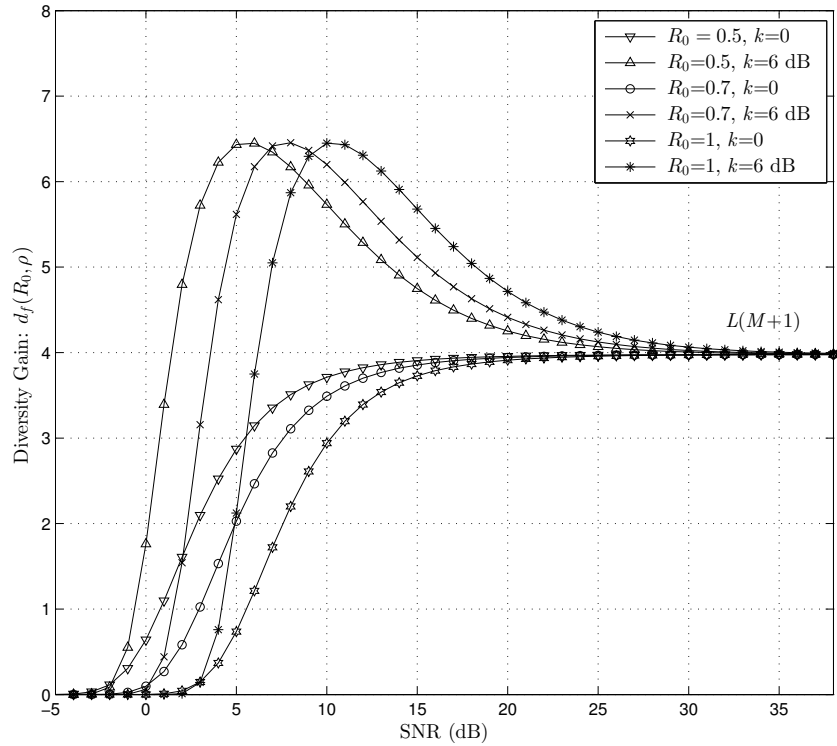


Figure 15: Diversity gain for different values of fixed transmission rate.

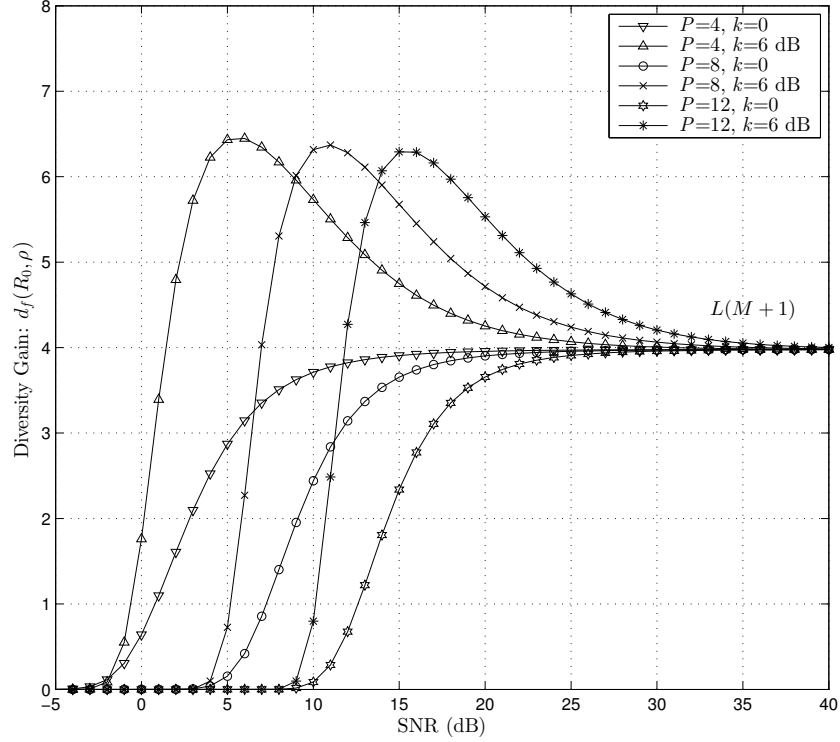


Figure 16: Diversity gain for different values of P at fixed transmission rate.

Fig. 17, shows the finite-SNR DMT (60) for $L = 2$, $N = 128$, $P = 4$, and $k = 6$ dB for a fixed SNR=10 dB. We consider various number of relay nodes $M = 1, 2, 3$. It is observed that by adding the number of relay nodes the diversity gain is increased for multiplexing gain $r_f = 0$. At $r_f = 0$, both Rician and Rayleigh fading channels achieve the same diversity gains, i.e., 2.48, 3.73, and 5 for $M = 1, 2, 3$, respectively. However, as opposed to Rayleigh fading channels in which the maximum achievable diversity gain always occurs at zero multiplexing gains, the maximum diversity gains over Rician fading channels are obtained at specific multiplexing gains. Specifically, maximum diversity gains of 2.78, 4.28, 5.6 are obtained at $r_f = 0.06, 0.07, 0.09$ for $M = 3, 2, 1$ respectively. Furthermore, for a zero diversity gain, we observe that maximum multiplexing gains are equal to 0.4, 0.33, 0.28 for $M = 1, 2, 3$, confirming the accuracy of (55).

Fig. 18 represents the finite-SNR DMT (60) for $L = 2$, $N = 128$, $P = 4$, $M = 1$,

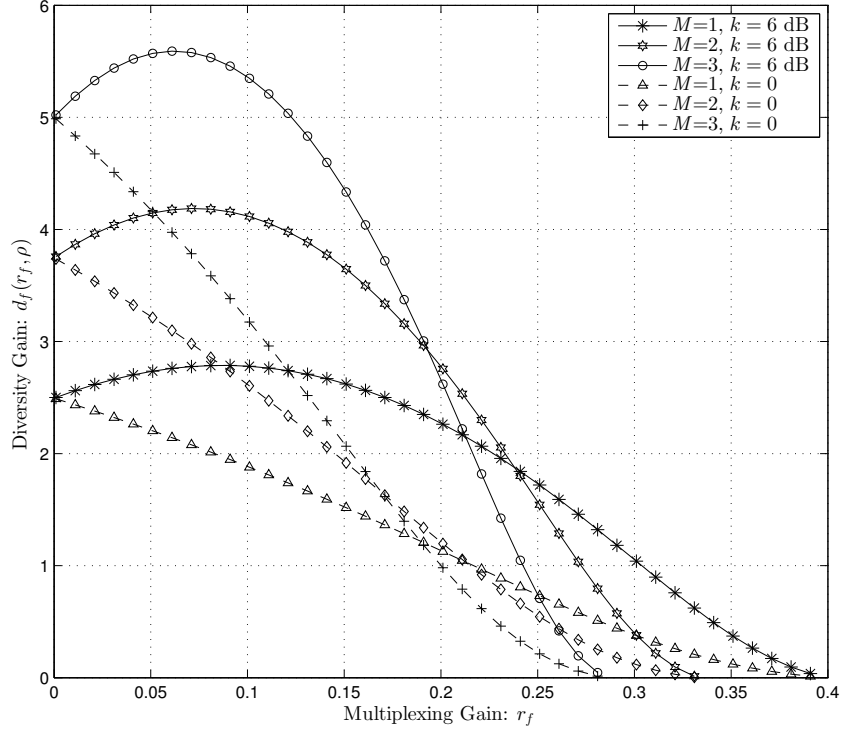


Figure 17: Finite-SNR DMT for different values of M .

and $k = 6$ dB. We consider various values of SNR=10, 20, 30 dB. It is observed that over Rayleigh fading channels increasing SNR leads to higher diversity gain throughout multiplexing range. However, for Rician fading channels, increasing SNR does not guarantee to have a higher diversity gain in the multiplexing range. For example, at some multiplexing gain values, it is possible to achieve a higher diversity gain at SNR=10 dB in comparison to that of SNR=30 dB. When SNR increases, the DMT curve approaches to $d(r) = 4(1 - 2.5r)$, c.f. Eq. (55), for both Rayleigh and Rician fading channels. Therefore, the asymptotic DMT is determined by number of coherence bandwidths as well as number of relay nodes.

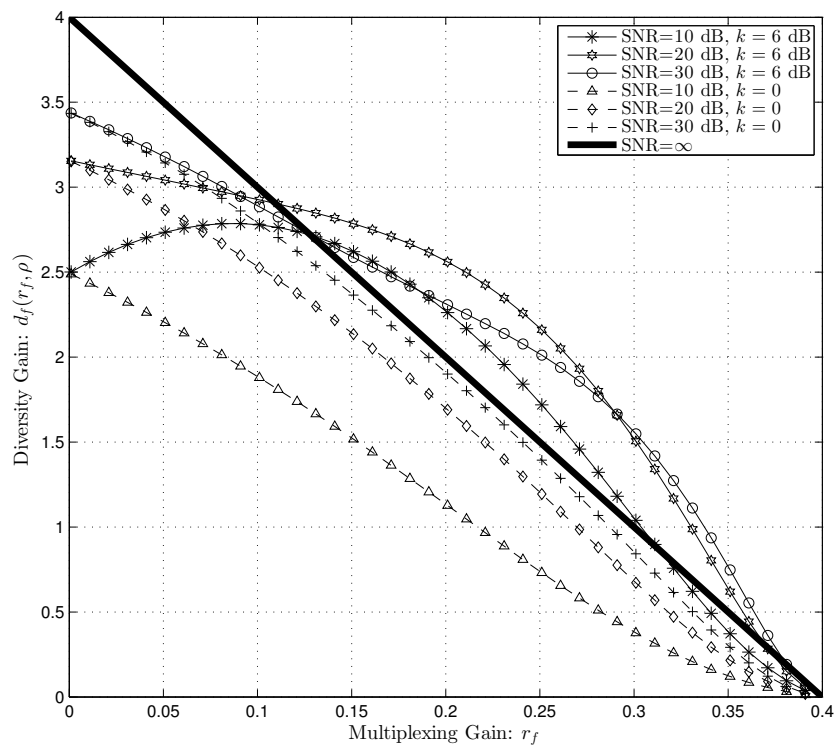


Figure 18: Finite-SNR DMT for different values of SNR.

CHAPTER V

CONCLUSION

In this thesis we have worked on the information theoretical performance analysis of NCC systems. In the first part of the thesis, we investigated the performance of NCC systems in the presence of imperfect CSI. Based on the derived outage probability, we obtained closed-form expression for finite-SNR DMT. Our results revealed that at practical channel estimation quality and SNR regime, the DMT of the system is substantially less than that of asymptotic one. This analysis can be useful to predict the performance of NCC system under realistic operating conditions taking into account channel estimation errors and finite SNR regime.

In the second part of the thesis, we have extended the DMT analysis of [10] presented for single-carrier TDMA-based NCC systems to NCC-OFDMA systems. Specifically, we have considered a system with P sources, M relays and one destination and employed maximum constraint $\kappa_{1,K}$ -matching approach for subcarrier allocation. We derived a closed-form expression for the outage probability of the system over fading channel and present the asymptotic DMT analysis. Our results demonstrated that NCC-OFDMA system is able to fully exploit both frequency and spatial diversity.

In the third part of the thesis, we derived finite-SNR DMT of NCC-OFDMA system over Rician fading channels. As opposed to Rayleigh fading, over Rician fading channels, the maximum diversity gain does not occur at zero multiplexing gain. It can be observed from our results that the presence of LOS components in Rician fading leads diversity gains higher than asymptotic SNR values at some multiplexing gains and SNRs.

Bibliography

- [1] A. Sendonaris, E. Erkip, and B. Aazhang, "User cooperation diversity. part I. system description," *IEEE Transactions on Communications*, vol. 51, pp. 1927–1938, Nov 2003.
- [2] A. Sendonaris, E. Erkip, and B. Aazhang, "User cooperation diversity. part II. implementation aspects and performance analysis," *IEEE Transactions on Communications*, vol. 51, pp. 1939–1948, Nov 2003.
- [3] J. Laneman, D. Tse, and G. W. Wornell, "Cooperative diversity in wireless networks: Efficient protocols and outage behavior," *IEEE Transactions on Information Theory*, vol. 50, pp. 3062–3080, Dec 2004.
- [4] L. Zheng and D. Tse, "Diversity and multiplexing: a fundamental tradeoff in multiple-antenna channels," *IEEE Transactions on Information Theory*, vol. 49, pp. 1073–1096, May 2003.
- [5] R. Ahlswede, N. Cai, S.-Y. Li, and R. Yeung, "Network information flow," *IEEE Transactions on Information Theory*, vol. 46, pp. 1204–1216, Jul 2000.
- [6] Y. Wu, P. A. Chou, and S. Y. Kung, "Information exchange in wireless networks with network coding and physical-layer broadcast," Tech. Rep. MSR-TR-2004-78, Microsoft Research, August 2004.
- [7] Y. Chen, S. Kishore, and J. Li, "Wireless diversity through network coding," in *IEEE Wireless Communications and Networking Conference (WCNC)*, vol. 3, pp. 1681–1686, April 2006.
- [8] S. Katti, H. Rahul, W. Hu, D. Katabi, M. Medard, and J. Crowcroft, "XORs in the air: Practical wireless network coding," *IEEE/ACM Transactions on Networking*, vol. 16, pp. 497–510, June 2008.
- [9] C. Peng, Q. Zhang, M. Zhao, Y. Yao, and W. Jia, "On the performance analysis of network-coded cooperation in wireless networks," *IEEE Transactions on Wireless Communications*, vol. 7, pp. 3090–3097, August 2008.
- [10] H. Topakkaya and Z. Wang, "Wireless network code design and performance analysis using diversity-multiplexing tradeoff," *IEEE Transactions on Communications*, vol. 59, pp. 488–496, February 2011.
- [11] J. Laneman and G. Wornell, "Distributed space-time-coded protocols for exploiting cooperative diversity in wireless networks," *IEEE Trans. Inf. Theory*, vol. 49, pp. 2415–2425, Oct. 2003.
- [12] A. Bletsas, A. Khisti, D. P. Reed, and A. Lippman, "A simple cooperative diversity method based on network path selection," *IEEE J. Sel. Areas Commun.*, vol. 24, pp. 659–672, Mar. 2006.

- [13] H. Gacanin and F. Adachi, “Broadband analog network coding,” *IEEE Transactions on Wireless Communications*, vol. 9, pp. 1577–1583, May 2010.
- [14] X. Wang, Y. Xu, and Z. Feng, “Physical-layer network coding in OFDM system: Analysis and performance,” in *Conference on Communications and Networking in China (CHINACOM)*, pp. 139–143, Aug 2012.
- [15] B. Han, W. Wang, and M. Peng, “Optimal resource allocation for network coding in multiple two-way relay OFDM systems,” in *IEEE Wireless Communications and Networking Conference (WCNC)*, pp. 1642–1647, April 2012.
- [16] J. Tian, H. F. Chong, and Y.-C. Liang, “Network coding for intra-cell communications in OFDMA networks,” *IEEE Wireless Communications Letters*, vol. 4, pp. 70–73, Feb 2015.
- [17] M. Haddad, M. Debbah, and A. Hayar, “Diversity-multiplexing tradeoff for frequency fading channels with CSIT,” in *International Conference on Cognitive Radio Oriented Wireless Networks and Communications*, pp. 1–5, June 2006.
- [18] D. Tse and P. Viswanath, *Fundamentals of wireless communication*. Cambridge university press, 2005.
- [19] B. Bai, W. Chen, K. Ben Letaief, and Z. Cao, “Finite-SNR diversity-multiplexing tradeoff for OFDM channels,” in *IEEE International Conference on Communications (ICC)*, pp. 1–5, May 2010.
- [20] B. Bai, W. Chen, Z. Cao, and K. Letaief, “Achieving high frequency diversity with subcarrier allocation in OFDMA systems,” in *IEEE Global Telecommunications Conference*, pp. 1–5, Nov 2008.
- [21] B. Bai, W. Chen, K. Ben Letaief, and Z. Cao, “Diversity-multiplexing tradeoff in OFDMA systems: An H-matching approach,” *IEEE Transactions on Wireless Communications*, vol. 10, pp. 3675–3687, November 2011.
- [22] R. Narasimhan, “Finite-SNR diversity-multiplexing tradeoff for correlated Rayleigh and Rician MIMO channels,” *IEEE Transactions on Information Theory*, vol. 52, pp. 3965–3979, Sept 2006.
- [23] W.-Y. Shin, S.-Y. Chung, and Y. H. Lee, “Diversity-multiplexing tradeoff and outage performance for Rician MIMO channels,” *IEEE Transactions on Information Theory*, vol. 54, no. 3, pp. 1186–1196, 2008.
- [24] S. Loyka and G. Levin, “On finite-SNR diversity-multiplexing tradeoff,” in *IEEE Global Telecommunications Conference, 2007*, pp. 1456–1461, Nov 2007.
- [25] P. Liu and I.-M. Kim, “Performance analysis of bidirectional communication protocols based on decode-and-forward relaying,” *IEEE Transactions on Communications*, vol. 58, pp. 2683–2696, September 2010.

- [26] X. Lin, M. Tao, Y. Xu, and R. Wang, "Outage probability and finite-SNR diversity-multiplexing tradeoff for two-way relay fading channels," *IEEE Transactions on Vehicular Technology*, vol. 62, pp. 3123–3136, Sept 2013.
- [27] Z. Yi, M. Ju, and I.-M. Kim, "Outage probability and optimum power allocation for analog network coding," *IEEE Transactions on Wireless Communications*, vol. 10, pp. 407–412, February 2011.
- [28] L. Wang, Y. Cai, and W. Yang, "On the finite-SNR DMT of two-way AF relaying with imperfect CSI," *IEEE Wireless Communications Letters*, vol. 1, pp. 161–164, June 2012.
- [29] J. C. Park, I. Song, and Y. H. Kim, "Outage-optimal allocation of relay power for analog network coding with three transmission phases," *IEEE Communications Letters*, vol. 16, pp. 838–841, June 2012.
- [30] S. Yadav and P. Upadhyay, "Performance of three-phase analog network coding with relay selection in Nakagami-m fading," *IEEE Communications Letters*, vol. 17, pp. 1620–1623, August 2013.
- [31] S. Yadav and P. Upadhyay, "Finite-SNR diversity-multiplexing tradeoff for three-phase ANC with channel estimation errors," *IEEE Communications Letters*, vol. 18, pp. 817–820, May 2014.
- [32] M. Medard, "The effect upon channel capacity in wireless communications of perfect and imperfect knowledge of the channel," *IEEE Transactions on Information Theory*, vol. 46, no. 3, pp. 933–946, 2000.
- [33] R. Narasimhan, "Effect of channel estimation errors on diversity-multiplexing tradeoff in multiple access channels," in *IEEE Global Communications Conference (Globecom)*, pp. 1–5, 2006.
- [34] B. Hassibi and B. Hochwald, "How much training is needed in multiple-antenna wireless links?," *IEEE Transactions on Information Theory*, vol. 49, no. 4, pp. 951–963, 2003.
- [35] P. Banelli, "Theoretical analysis and performance of OFDM signals in nonlinear fading channels," *IEEE Transactions on Wireless Communications*, vol. 2, pp. 284–293, Mar 2003.
- [36] M. K. Simon and M.-S. Alouini, *Digital communication over fading channels*. John Wiley & Sons, 2005.
- [37] F. Bowman, *Introduction to Bessel functions*. Courier Corporation, 1958.
- [38] R. L. Graham, D. E. Knuth, and O. Patashnik, "Concrete mathematics (1989)," *Massachusetts: Addison-Wesley*.

VITA

Ali Reza Heidarpour received his B.Sc. degree in electrical engineering from University of Isfahan, Isfahan, Iran, in 2013. He is currently a M.Sc. student at Electrical and Electronic engineering department and a member of Communication Theory and Technology (CT&T) research group under supervision of Professor Murat Uysal at Ozyegin University, Istanbul, Turkey. His research is in the area of OFDMA systems, cooperative communication and diversity techniques.